

# Ligand-Gated Channels

- [Introduction to GABA Receptors](#)
- [References for GABA Receptors](#)

[GABAA  \$\alpha\$ 1/ \$\beta\$ 3/ \$\gamma\$ 2](#)  
[GABAA  \$\alpha\$ 2/ \$\beta\$ 3/ \$\gamma\$ 2](#)  
[GABAA  \$\alpha\$ 3/ \$\beta\$ 3/ \$\gamma\$ 2](#)  
[GABAA  \$\alpha\$ 4/ \$\beta\$ 3/ \$\gamma\$ 2](#)  
[GABAA  \$\alpha\$ 5/ \$\beta\$ 3/ \$\gamma\$ 2](#)  
[GABAA  \$\alpha\$ 6/ \$\beta\$ 3/ \$\gamma\$ 2](#)

- [Introduction to Nicotinic Acetylcholine Receptors](#)
- [References for Nicotinic Acetylcholine Receptors](#)

[nAChR  \$\alpha\$ 1/ \$\beta\$ 1/ \$\delta\$ / \$\epsilon\$](#)   
[nAChR  \$\alpha\$ 3/ \$\beta\$ 4](#)  
[nAChR  \$\alpha\$ 4/ \$\beta\$ 2](#)  
[nAChR  \$\alpha\$ 7/ \$\text{ric}3\$](#)

Click Channel Type to Access Validation Data:

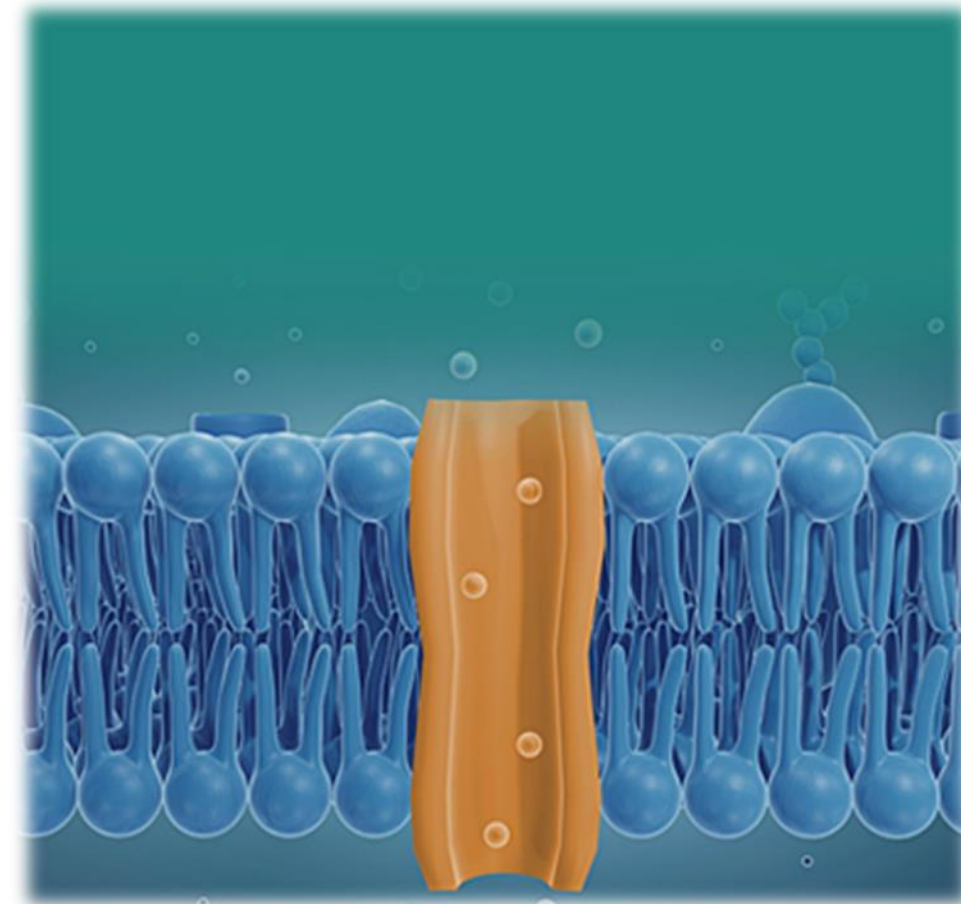
- [Introduction to Glycine Receptors](#)
- [References for Glycine Receptors](#)

[GlyRA1](#)

- [Introduction to Glutamate Receptors](#)
- [References for Glutamate Receptors](#)

[GluR6](#)

Please press the “Back” button to return to the previous menu



[BACK](#)

GABA<sub>A</sub> receptors are anion channels opened by  $\gamma$ -aminobutyric acid (GABA). Based on their amino acid sequences they belong to the same superfamily as the glycine receptors, anionic glutamate receptors, nicotinic acetylcholine receptors, and the 5-HT<sub>3</sub> receptor [1]. Each functional GABA channel molecule contains five subunits. There are at least 19 distinct but related GABA<sub>A</sub> receptor subunits in mammals. Alternative exon splicing of the pre-mRNA forms even more heterogeneity.

The five subunit GABA<sub>A</sub> receptors in the central nervous system produce combinations of  $\alpha$  and  $\beta$  subunits plus one or more of the  $\gamma$ ,  $\delta$ ,  $\theta$ ,  $\pi$  or  $\epsilon$  subunit types [2]. The majority contain only the  $\alpha\beta\gamma$  combination. In addition there are three known  $\rho$  subunits that occur mainly in the retina and which appear to assemble separately from all others.

GABA<sub>A</sub> receptors possess a large and varied set of modulatory sites where ligands modify the response to GABA [3]. Selective ligands at these sites differentiate a series of subtypes for the GABA<sub>A</sub> receptor.

The modulatory benzodiazepine site offers distinct pharmacology for the definition of subtypes of the GABA<sub>A</sub> receptors. The majority of GABA<sub>A</sub> receptors carry some form of the benzodiazepine site. Benzodiazepines generally enhance the action of GABA, but some ligands act in the opposite direction at the benzodiazepine site.

There are many other distinct modulatory sites that have been found on GABA<sub>A</sub> receptors [4,5,6], some ligands show a preference for particular subunit isoforms or subunit combinations.

- 1) Barnard EA. (1996) The transmitter-gated channels: a range of receptor types and structures. *Trends Pharmacol Sci*, **17** (9): 305-9. [PMID:8885692]
- 2) Bencsits E, Ebert V, Tretter V, Sieghart W. (1999) A significant part of native gamma-aminobutyric AcidA receptors containing alpha4 subunits do not contain gamma or delta subunits. *J Biol Chem*, **274** (28): 19613-6. [PMID:10391897]
- 3) Macdonald RL, Olsen RW. (1994) GABAA receptor channels. *Annu Rev Neurosci*, **17**: 569-602. [PMID:7516126]
- 4) Barnard EA, Skolnick P, Olsen RW, Mohler H, Sieghart W, Biggio G, Braestrup C, Bateson AN, Langer SZ. (1998) International Union of Pharmacology. XV. Subtypes of gamma-aminobutyric acidA receptors: classification on the basis of subunit structure and receptor function. *Pharmacol Rev*, **50** (2): 291-313. [PMID:9647870]
- 5) Macdonald RL, Olsen RW. (1994) GABAA receptor channels. *Annu Rev Neurosci*, **17**: 569-602. [PMID:7516126]
- 6) Sieghart W. (1995) Structure and pharmacology of gamma-aminobutyric acidA receptor subtypes. *Pharmacol Rev*, **47** (2): 181-234. [PMID:7568326]

[BACK](#)

# Introduction to Nicotinic Acetylcholine Receptors

[BACK](#)

Nicotinic acetylcholine receptors (nAChRs) are multi-subunit transmembrane neurotransmitter receptors that are classified in the 'Cys-loop' superfamily [1,2]. They are found in the central and peripheral nervous systems, as well as the non-neuronal cholinergic system [3,4]. nAChRs contain five subunits, assemble in both heteromeric and homomeric pentamers and at least sixteen subunits in mammals have been found [5].

nAChRs mediate ionotropic effects of the neurotransmitter acetylcholine. nAChRs are involved in excitatory neurotransmission at the neuromuscular junction, in the autonomic nervous system, and at particular synapses in the brain and spinal cord [1,3].

Expression of certain nAChRs in brain and muscle is developmentally regulated [6,7,8]. Some nAChRs are expressed in a variety of other tissues and cell types as well as sensory organs [4]. nAChRs may serve a modulatory function in these cells [9,10].

nAChR subunits are homologous, sharing the same topographical features as subunits of other 'Cys-loop' receptors such as GABA and 5-HT receptors, ionotropic glycine, and some glutamate-gated Cl<sup>-</sup> channels. These features include four transmembrane segments, a large extracellular N-terminal domain, a cytoplasmic loop of variable length, and a short extracellular C-terminus [7].

Autonomic neurons express  $\alpha 3\beta 4^*$  where asterisk denotes they may include other subunits in this case including  $\alpha 5$ ,  $\beta 2$  and  $\alpha 7$  nAChRs. Brain and spinal cord neurons express various combinations of subunits, with  $\alpha 4\beta 2^*$  and  $\alpha 7$  nAChRs predominating.

# References for nAChR's

- 1) Albuquerque EX, Pereira EF, Alkondon M, Rogers SW. (2009) Mammalian nicotinic acetylcholine receptors: from structure to function. *Physiol Rev*, **89** (1): 73-120. [PMID:19126755]
- 2) Sine SM, Engel AG. (2006) Recent advances in Cys-loop receptor structure and function. *Nature*, 440 (7083): 448-55. [PMID:16554804]
- 3) Dani JA, Bertrand D. (2007) Nicotinic acetylcholine receptors and nicotinic cholinergic mechanisms of the central nervous system. *Annu Rev Pharmacol Toxicol*, 47: 699-729. [PMID:17009926]
- 4) Wessler I, Kirkpatrick CJ. (2008) Acetylcholine beyond neurons: the non-neuronal cholinergic system in humans. *Br J Pharmacol*, 154 (8): 1558-71. [PMID:18500366]
- 5) Millar NS, Gotti C. (2009) Diversity of vertebrate nicotinic acetylcholinereceptors. *Neuropharmacology*, 56 (1): 237-46. [PMID:18723036]
- 6) Campbell NR, Fernandes CC, Half AW, Berg DK. (2010) Endogenous signaling through alpha7-containing nicotinic receptors promotes maturation and integration of adult-born neurons in the hippocampus. *J Neurosci*, 30 (26): 8734-44. [PMID:20592195]
- 7) Karlin A. (2002) Emerging structure of the nicotinic acetylcholine receptors. *Nat Rev Neurosci*, 3 (2): 102-14. [PMID:11836518]
- 8) Liu Z, Zhang J, Berg DK. (2007) Role of endogenous nicotinic signaling in guiding neuronal development. *Biochem Pharmacol*, 74 (8): 1112-9. [PMID:17603025]
- 9) Arias HR, Richards VE, Ng D, Ghafoori ME, Le V, Mousa SA. (2009) Role of non-neuronal nicotinic acetylcholine receptors in angiogenesis. *Int J Biochem Cell Biol*, **41** (7): 1441-51. [PMID:19401144]
- 10) Grando SA. (2008) Basic and clinical aspects of non-neuronal acetylcholine: biological and clinical significance of non-canonical ligands of epithelial nicotinic acetylcholine receptors. *J Pharmacol Sci*, **106** (2): 174-9. [PMID:18285656]

[BACK](#)

# Introduction to Glycine Receptors

The glycine receptor Cl<sup>-</sup> channel (GlyR) mediates inhibitory synaptic transmission in reflex circuits of the spinal cord. Glycine was found to be an inhibitory neurotransmitter from an analysis of its distribution in the spinal cord [1]. Glycine activates a strychnine-sensitive Cl<sup>-</sup> conductance in spinal cord neurons [2-4]. The  $\alpha$ 1 GlyR subunit was cloned in 1987 [5] and due to its homology with the nAChRs it is part of the Cys-loop family of ligand-gated ion channel receptors. GlyR's are also found pre-synaptically, where they modulate neurotransmitter release.

[BACK](#)

GlyRs are pentameric assemblies around an ion-conducting pore. Similar to other Cys-loop receptor subunits, each GlyR subunit has a large extracellular amino-terminal domain that includes the ligand binding sites.

Amino acid agonists at GlyRs rank order potency is glycine >  $\beta$ -alanine > taurine. The only non-peptidic agonist identified so far is ivermectin [14]. GlyRs are antagonised by strychnine in a potent and specific manner. Picrotoxin distinguishes between  $\alpha$  homomeric and  $\alpha\beta$  heteromeric GlyRs [6]. Much current therapeutic research is focused on the development of GlyR-specific drugs for movement disorders and chronic inflammatory pain.

# References for Glycine Receptors

- 1) Aprison MH, Werman R. (1965) The distribution of glycine in cat spinal cord and roots. *Life Sci*, **4** (21): 2075-83. [PMID:5866625]
- 2) Callister RJ, Graham BA. (2010) Early history of glycine receptor biology in Mammalian spinal cord circuits. *Front Mol Neurosci*, **3**: 13. [PMID:20577630]
- 3) Curtis DR, Hösl L, Johnston GA. (1967) Inhibition of spinal neurons by glycine. *Nature*, **215** (5109): 1502-3. [PMID:4293850]
- 4) Werman R, Davidoff RA, Aprison MH. (1967) Inhibition of motoneurons by iontophoresis of glycine. *Nature*, **214** (5089): 681-3. [PMID:4292803]
- 5) Grenningloh G, Rienitz A, Schmitt B, Methfessel C, Zensen M, Beyreuther K, Gundelfinger ED, Betz H. (1987) The strychnine-binding subunit of the glycine receptor shows homology with nicotinic acetylcholine receptors. *Nature*, **328** (6127): 215-20. [PMID:3037383]
- 6) Pribilla I, Takagi T, Langosch D, Bormann J, Betz H. (1992) The atypical M2 segment of the beta subunit confers picrotoxinin resistance to inhibitory glycine receptor channels. *EMBO J*, **11** (12): 4305-11. [PMID:1385113]

[BACK](#)

# Introduction to Glutamate Receptors

[BACK](#)

The ionotropic glutamate receptors include NMDA, AMPA, and kainate receptor classes, named originally according to their agonist [1-3]. Receptors are comprised of homo- or hetero-oligomeric subunits assembled into cation-selective tetramers.

GluR6 is a kainate receptor now more commonly known as the GluK2 receptor. Kainate receptors can be expressed as homomers or heterotetramers of GluK1, GluK2 or GluK3 subunits. [4-6]). Kainate receptors require extracellular  $\text{Na}^+$  and  $\text{Cl}^-$  for their activation [7-8].

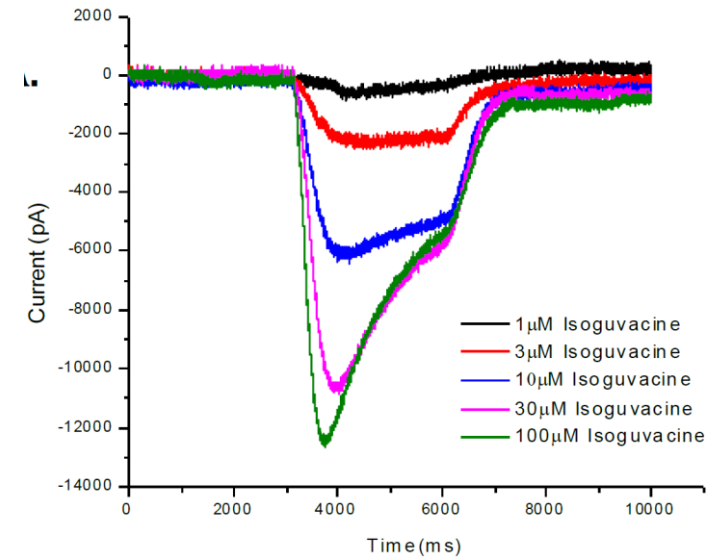
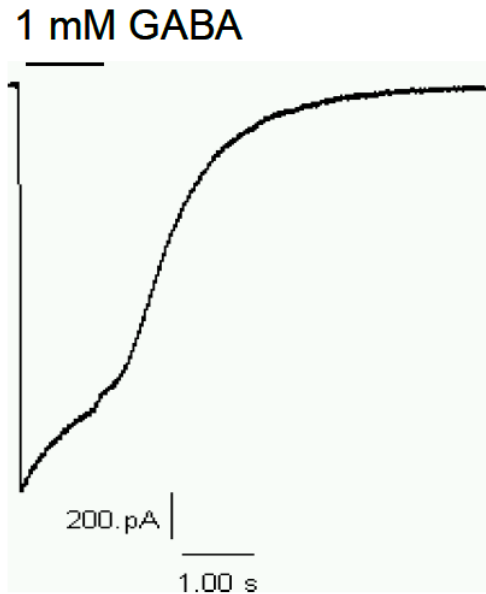


# References for Glutamate Receptors

[BACK](#)

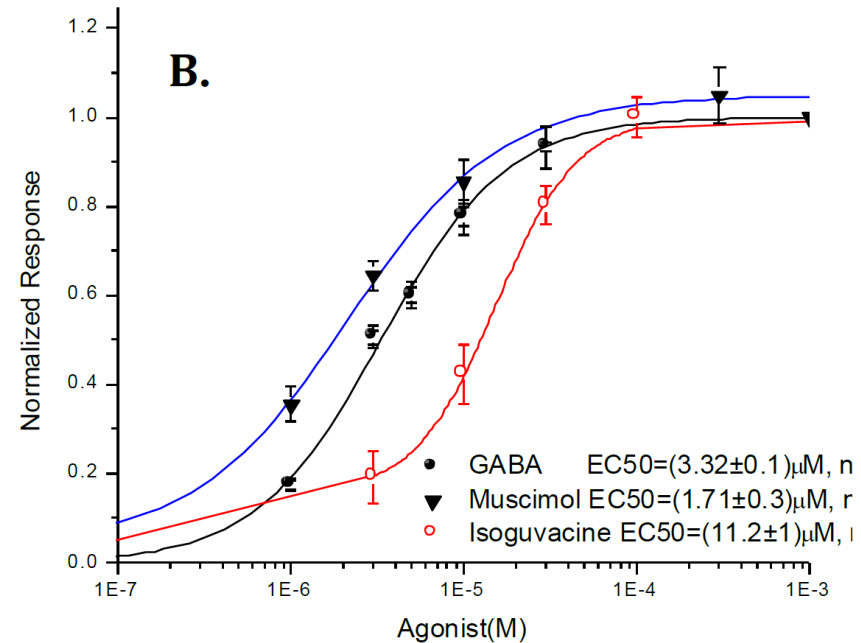
- 1) Dingledine R, Borges K, Bowie D, Traynelis SF. (1999) The glutamate receptor ion channels. *Pharmacol Rev*, **51** (1): 7-61. [PMID:10049997]
- 2) Lodge D. (2009) The history of the pharmacology and cloning of ionotropic glutamate receptors and the development of idiosyncratic nomenclature. *Neuropharmacology*, **56** (1): 6-21. [PMID:18765242]
- 3) Traynelis SF, Wollmuth LP, McBain CJ, Menniti FS, Vance KM, Ogden KK, Hansen KB, Yuan H, Myers SJ, Dingledine R. (2010) Glutamate receptor ion channels: structure, regulation, and function. *Pharmacol Rev*, **62** (3): 405-96. [PMID:20716669]
- 4) Lerma J. (2006) Kainate receptor physiology. *Curr Opin Pharmacol*, **6** (1): 89-97. [PMID:16361114]
- 5) Perrais D, Veran J, Mulle C. (2010) Gating and permeation of kainate receptors: differences unveiled. *Trends Pharmacol Sci*, **31** (11): 516-22. [PMID:20850188]
- 6) Pinheiro P, Mulle C. (2006) Kainate receptors. *Cell Tissue Res*, **326** (2): 457-82. [PMID:16847640]
- 7) Bowie D. (2010) Ion-dependent gating of kainate receptors. *J Physiol (Lond.)*, **588** (Pt 1): 67-81. [PMID:19822544]
- 8) Plested AJ. (2011) Kainate receptor modulation by sodium and chloride. *Adv Exp Med Biol*, **717**: 93-113. [PMID:21713670]

BACK



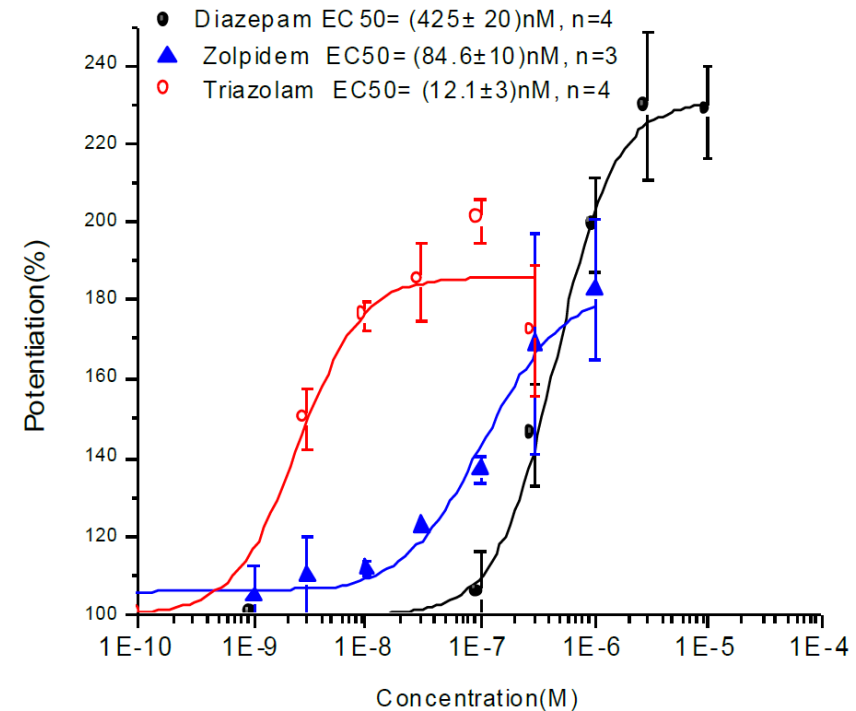
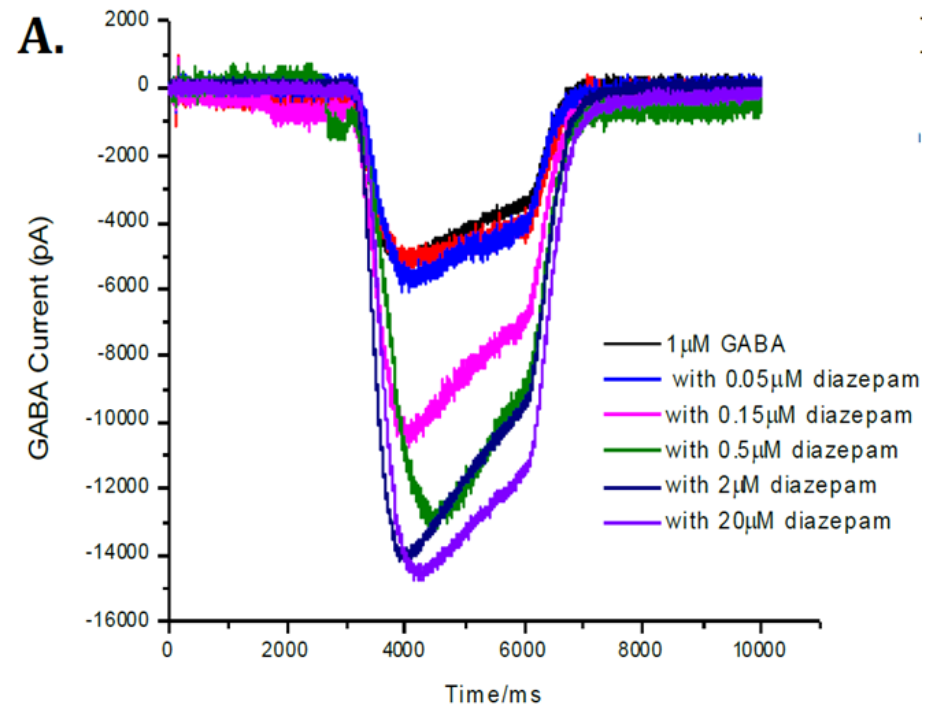
**hGABAA  $\alpha$ 1/ $\beta$ 3/ $\gamma$ 2 Current Activation by Agonist:** **Left:** Typical current trace upon addition of 1 mM GABA. (Manual Patch Clamp Data) **Right:** Example of typical GABAA  $\alpha$ 1 currents activated by increasing concentrations of isoguvacine, a GABA receptor agonist, applied for 3 s at increasing doses from 1  $\mu$ M to 100  $\mu$ M. (IonFluxHT Data)

BACK



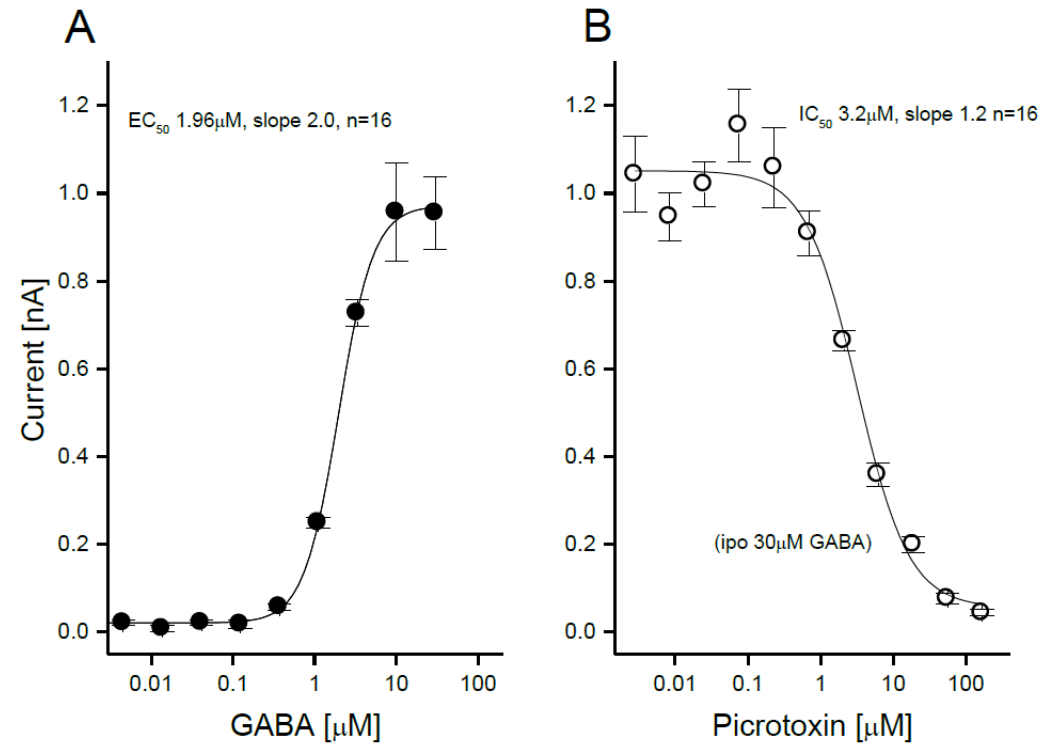
**hGABAA  $\alpha$ 1/ $\beta$ 3/ $\gamma$ 2 Current Activation by Agonist:** Comparison of dose-response curves for three agonists: GABA, isoguvacine, and muscimol. Hill fits yield  $EC_{50}$  values of 3.3, 11.2, and 1.7  $\mu M$  respectively, in good agreement with literature. (IonFlux HT Data)

BACK



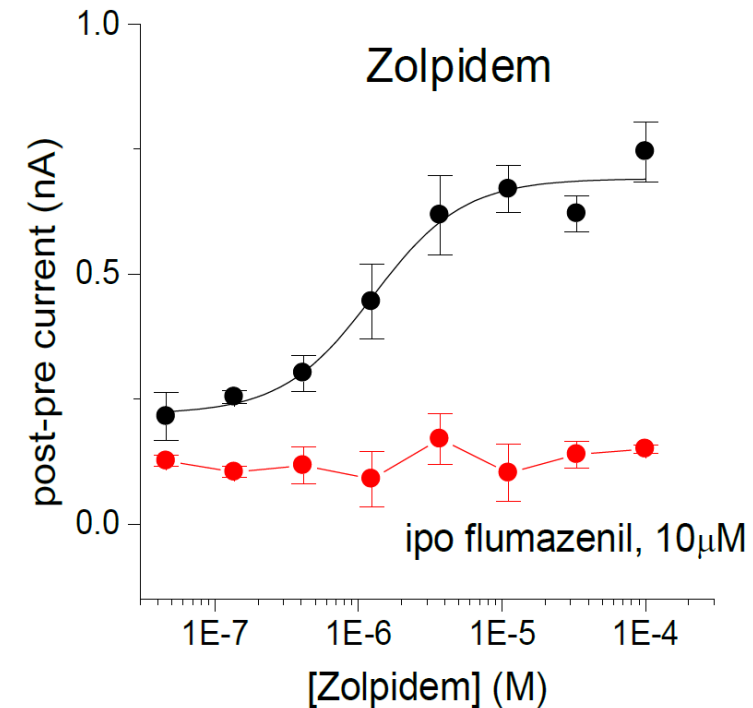
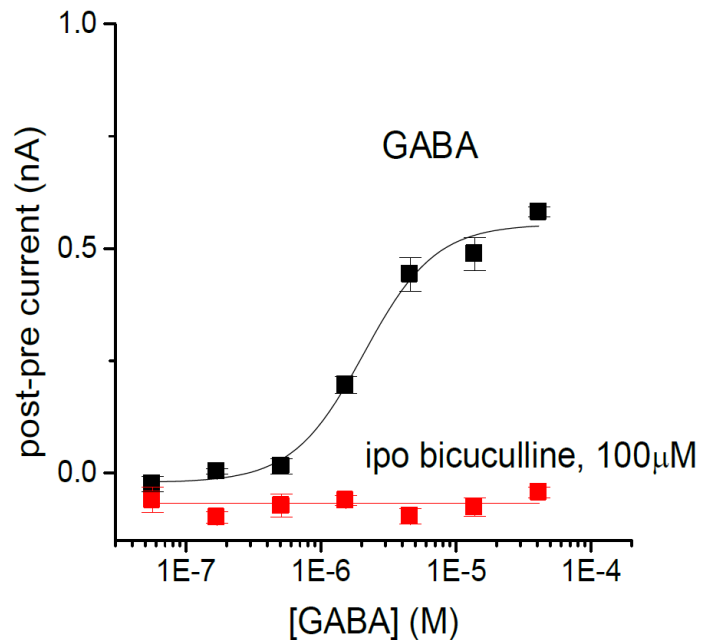
**hGABAA  $\alpha 1/\beta 3/\gamma 2$  Positive Allosteric Modulator Response:** **Left:** Response of a cell ensemble exposed to 1  $\mu$ M GABA ( $EC_{20}$ ) with pre-incubated and co-applied with increasing diazepam concentrations. **Right:** Dose response analysis yielded  $EC_{50}$  of diazepam 425nM ( $n=4$ , hill slope= 1.28,  $R^2= 0.977$ ). The reported literature  $EC_{50}$  value is ~160nM.  $EC_{50}$  of zolpidem was 84.6nM ( $n=3$ , hill slope= 1.25  $R^2=0.967$ ). The reported literature  $EC_{50}$  values range from 70nM to 150nM.  $EC_{50}$  of triazolam was 12.1nM ( $n=4$ , hill slope =1.41,  $R^2=0.970$ ). The reported literature  $EC_{50}$  values range from 22nM to 45nM (IonFlux HT Data).

BACK



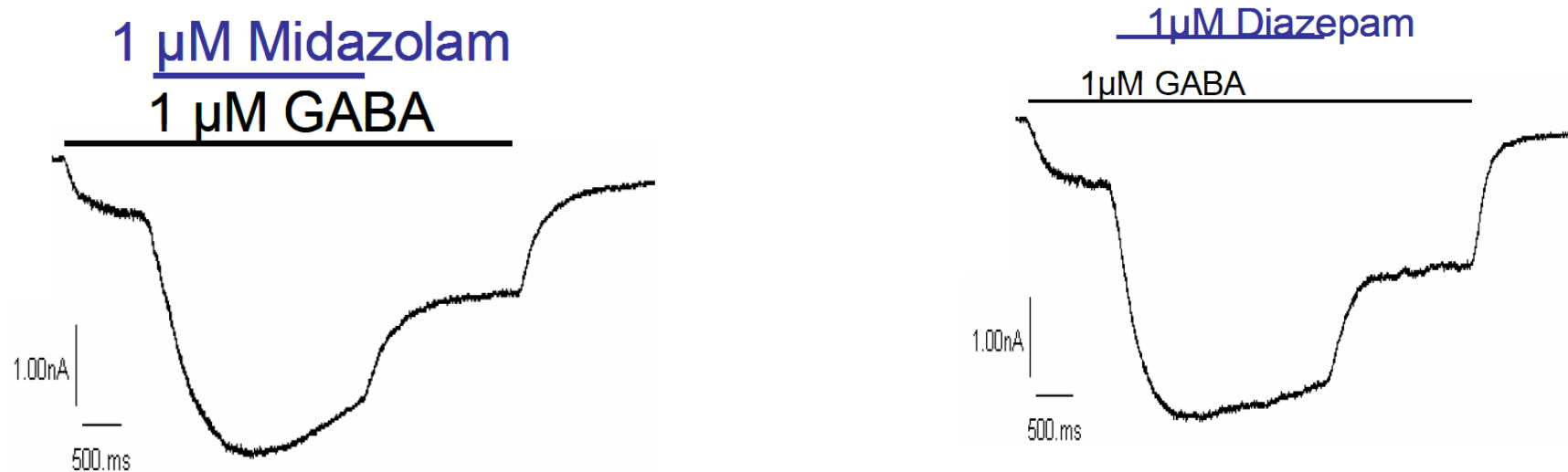
**hGABAA  $\alpha$ 1/ $\beta$ 3/ $\gamma$ 2 Agonist and Antagonist Dose Response Curves:** Activation by GABA (left) and inhibition by Picrotoxin (right) of the 30  $\mu$ M GABA response (IonWorks Quattro Data).

BACK



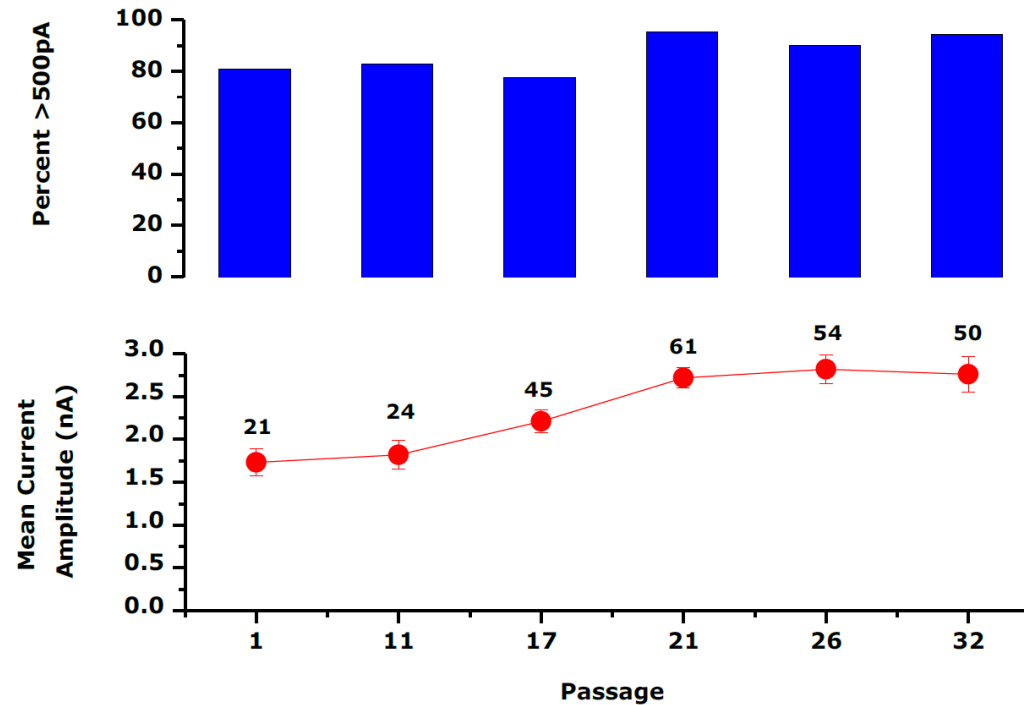
**hGABAA  $\alpha$ 1/ $\beta$ 3/ $\gamma$ 2 Bicuculline Inhibition of GABA responses, Potentiation of GABA Response by Zolpidem and Block by Flumazenil:** **Left:** GABA concentration response with a mean  $EC_{50}$  value of 1.96  $\mu$ M (n=16) and a slope (k) of 2.0. Bicuculline, a known GABA antagonist, abolished (>98% block at 11  $\mu$ M) responses to 10  $\mu$ M GABA. It was also further demonstrated that a single dose (100  $\mu$ M) of bicuculline completely inhibited the currents across a full GABA dose response curve. **Right:** In addition it was shown that the benzodiazepine zolpidem potentiated the 1  $\mu$ M GABA signal with an approximate  $EC_{50}$  of 2  $\mu$ M. This positive modulation was blocked by 10  $\mu$ M flumazenil (IonWorks Quattro Data).

BACK



**Potentiation of hGABAA  $\alpha$ 1/ $\beta$ 3/ $\gamma$ 2 Currents by the Benzodiazepines Midazolam and Diazepam:** In order to verify the co-expression of the  $\gamma$ 2 subunit, the benzodiazepine midazolam (**left**) was tested on the currents evoked by GABA (1  $\mu$ M, EC20) using conventional patch clamp. 1  $\mu$ M midazolam augmented this GABA response by  $462 \pm 88\%$  (mean  $\pm$  SEM). The 1  $\mu$ M GABA response was also augmented by diazepam (**right**) (Manual Patch Clamp Data).

BACK

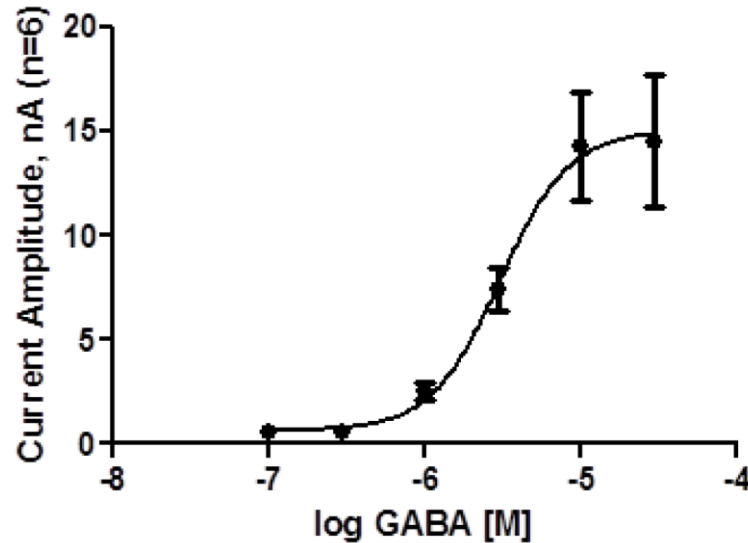


**hGABAA  $\alpha$ 1/ $\beta$ 3/ $\gamma$ 2 Stability of Expression Over Passage:** The upper panel shows the percentage of cells expressing a mean peak current >500 pA at 0 mV at cell passages 1, 11, 17, 21, 26 and 32. The lower panel shows the mean current amplitude (mean  $\pm$  SEM, red circles) and the number of these cells (IonWorks HT Data).

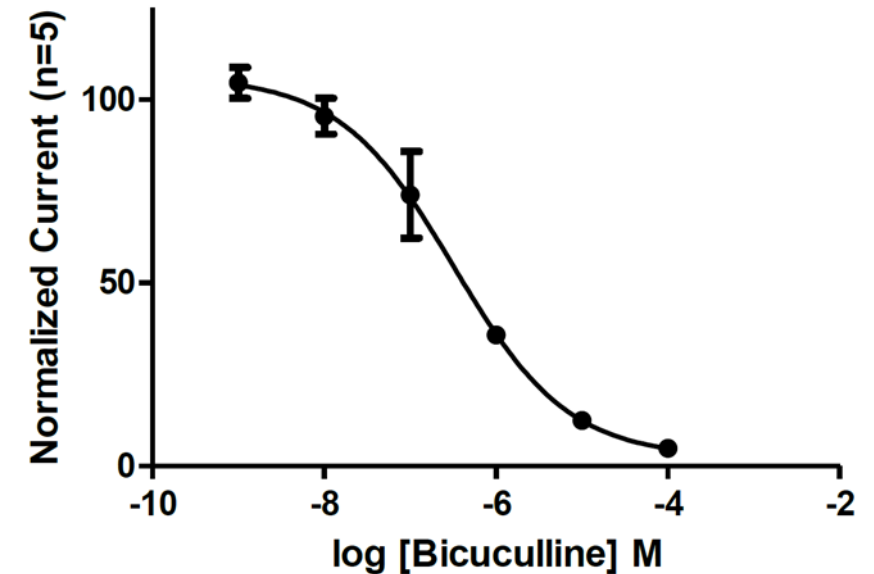


# hGABAA $\alpha 2/\beta 3/\gamma 2$ (CYL3072)

BACK

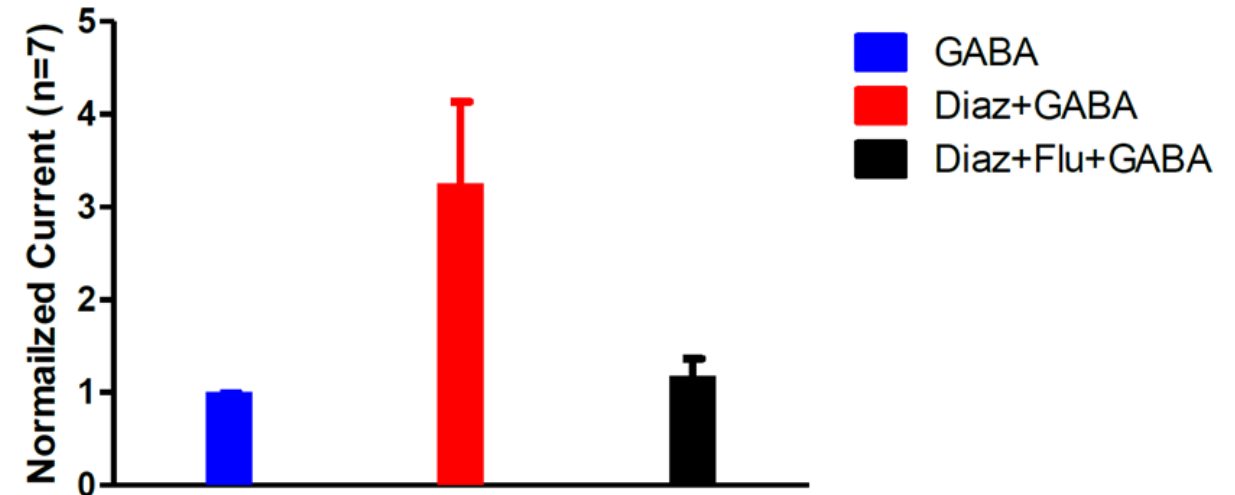
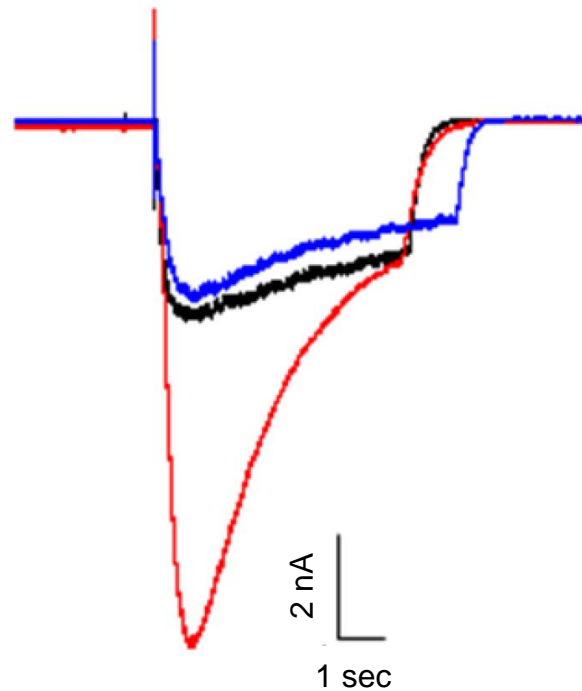


Passage	EC50 ( $\mu$ M)	EC20 ( $\mu$ M)	EC80 ( $\mu$ M)
11	3.71 $\pm$ 1.26	2.27 $\pm$ 0.70	6.57 $\pm$ 3.84
20	3.06 $\pm$ 1.12	1.51 $\pm$ 0.78	6.19 $\pm$ 1.77
25	3.31 $\pm$ 2.00	1.54 $\pm$ 0.96	8.59 $\pm$ 3.84
32	2.80 $\pm$ 1.21	1.17 $\pm$ 0.71	7.11 $\pm$ 2.98



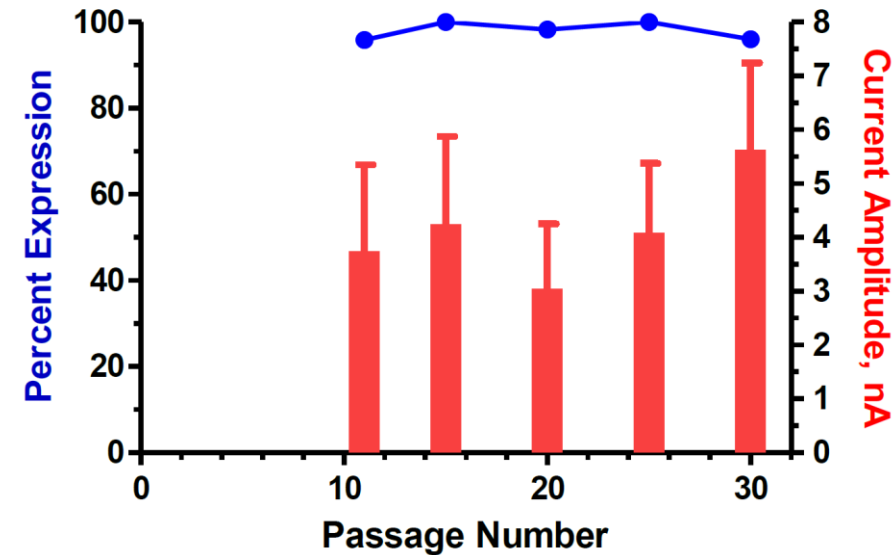
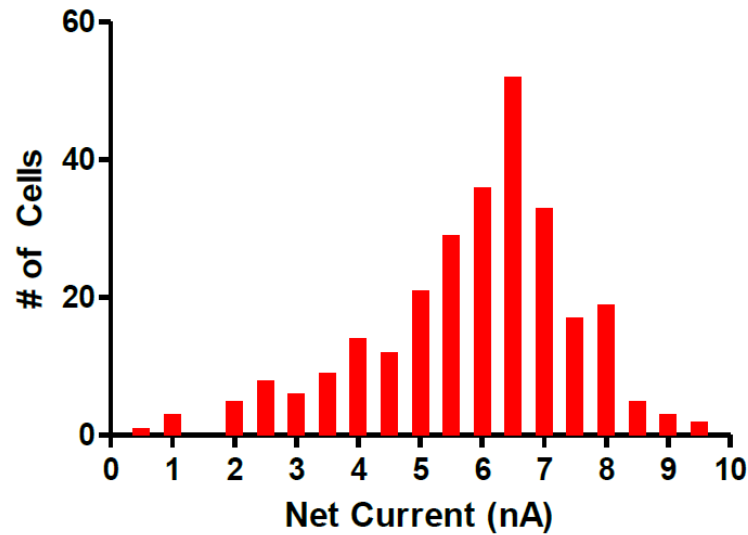
**hGABAA  $\alpha 2/\beta 3/\gamma 2$  Agonist and Antagonist Dose Response Curves:** **Left:** GABA concentration-response curve for hGABAA  $\alpha 2/\beta 3/\gamma 2$ -HEK cells at passage 20. **Middle:** Assays designed to detect novel allosteric modulators often employ protocols where the test compound is added with a fixed concentration of GABA. The table shows the reproducibility of the GABA EC<sub>50</sub>, EC<sub>20</sub> and EC<sub>80</sub> values (mean  $\pm$  SD) with increasing passage number. Each point indicates the mean ( $\pm$ ) response for 6 cells. We obtained an EC<sub>50</sub> of 3.06  $\mu$ M and a Hill slope of 1.96. **Right:** Bicuculline inhibition of response to addition of GABA at the EC<sub>80</sub> concentration. Each point indicates the response of 5 cells. We obtained an IC<sub>50</sub> of 0.324  $\mu$ M and a Hill slope of -0.652. (PatchXpress Data).

BACK



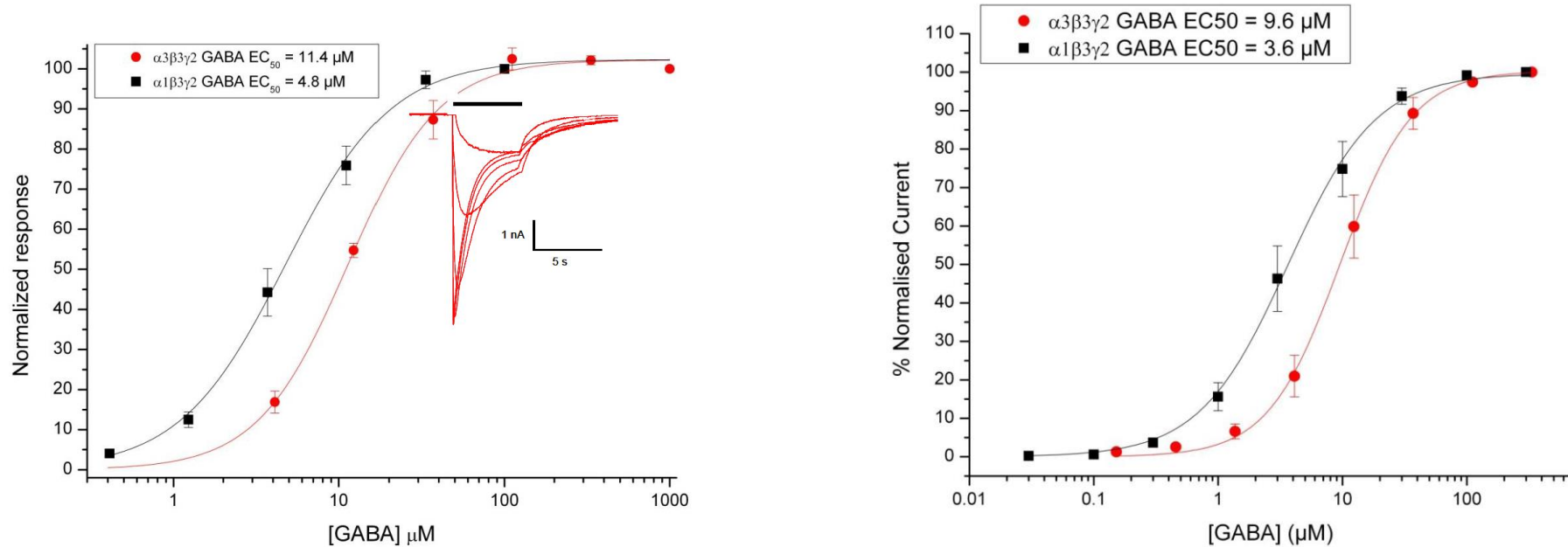
**hGABAA  $\alpha 2/\beta 3/\gamma 2$  Effect of Diazepam and Flumazenil:** **Left:** The response of a single representative cell is shown. The blue trace shows the response to the addition of an EC<sub>20</sub> concentration of GABA. After washout, 1 μM diazepam was added alone and had no effect (not shown). After a 2 min incubation with 1 μM diazepam, the response to the addition of an EC<sub>20</sub> concentration of GABA+diazepam (red trace) was now enhanced. The effect of 1 μM diazepam was completely blocked by 10 μM flumazenil (black trace), indicating the effect is mediated through the benzodiazepine binding site on the GABA A  $\alpha 2/\beta 3/\gamma 2$  receptor. **Right:** The combined data for seven cells are shown graphically in the bar chart below (PatchXpress Data).

BACK



**hGABAA  $\alpha 2/\beta 3/\gamma 2$  Current Amplitudes and Stability over Passages:** **Left:** Frequency distribution of current amplitude obtained in single-hole mode. The GABAA  $\alpha 2/\beta 3/\gamma 2$  current was defined as the peak current post GABA (100 $\mu$ M) addition minus the peak current pre GABA addition with a minimum acceptable current of 500pA. **Right:** Stability of expression and current amplitude. The blue line shows the percentage of cells expressing a mean peak inward current >0.5 nA at -40 mV at cell passages 11, 15, 20, 25 and 30. The red bars show the mean current amplitude (mean  $\pm$  SD) for 73-269 cells per experiment (IonWorks Quattro Data).

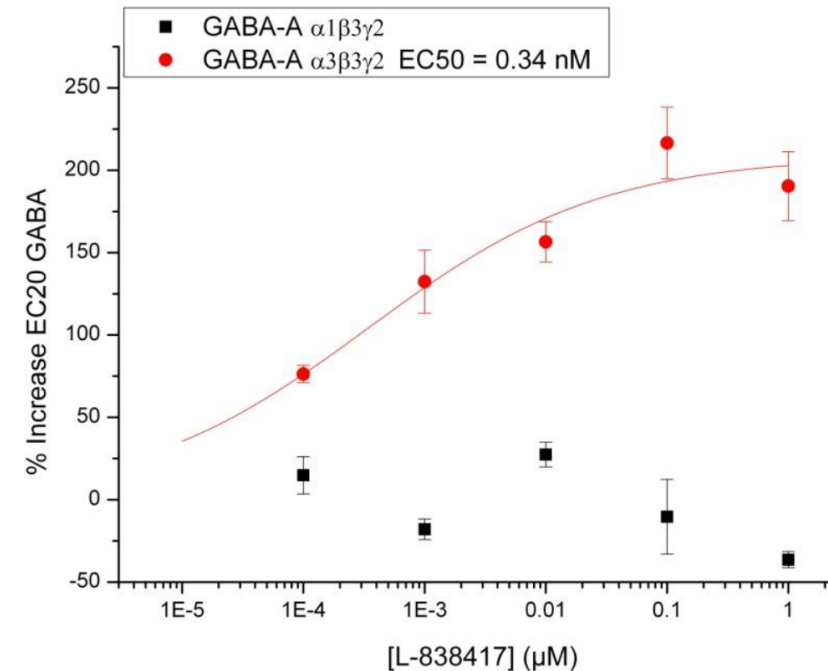
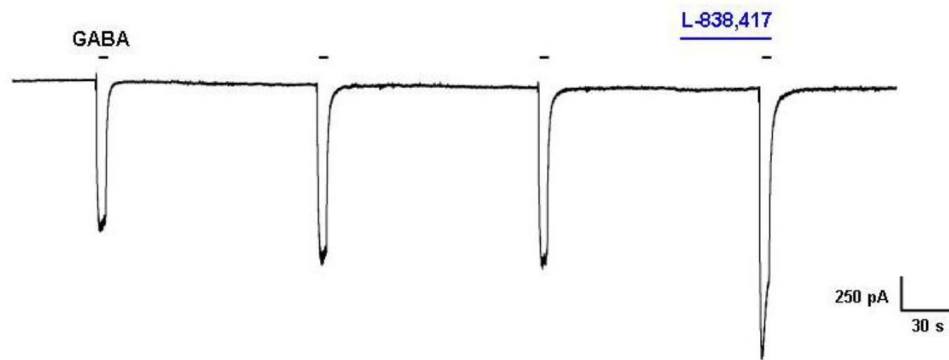
BACK



## hGABAA $\alpha 3/\beta 3/\gamma 2$ Dose-Response Curve Compared to GABA $\alpha 1$ on Two Different Automated Electrophysiology

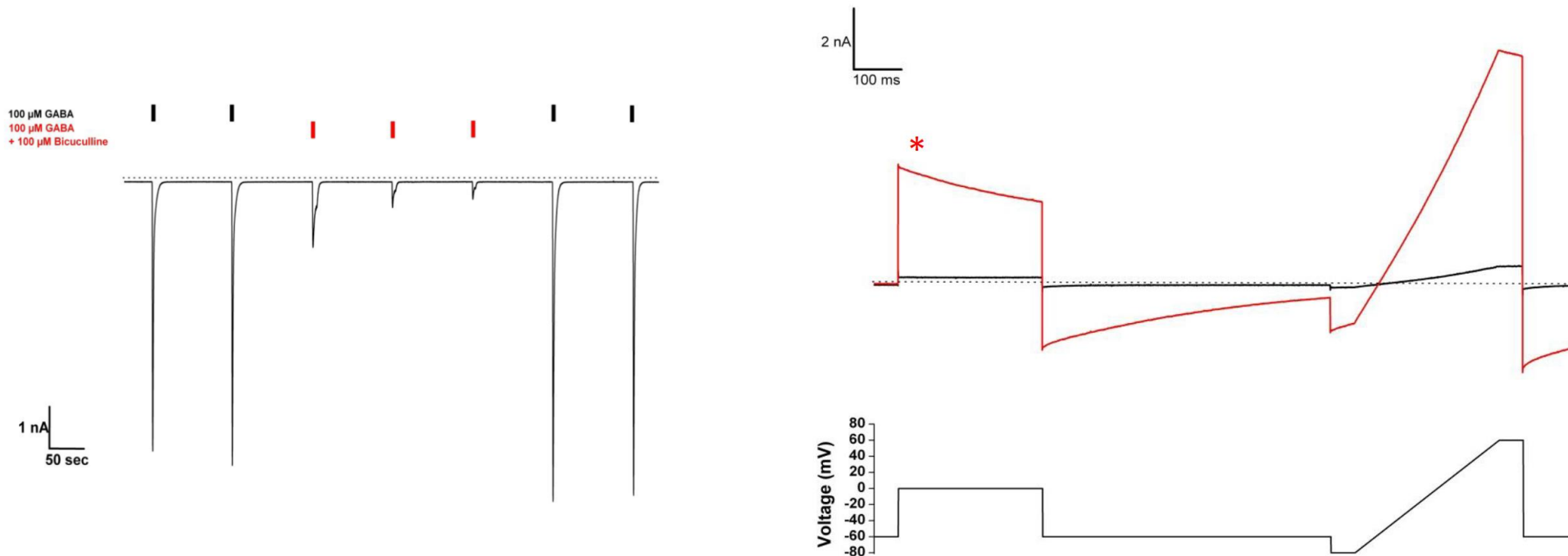
**Platforms:** **Left:** GABA concentration-response curves for  $\alpha 1$  (black squares) and  $\alpha 3$  (red circles). **Left Inset:** Example of typical GABA A  $\alpha 3$  currents activated by increasing concentrations of GABA applied for 5 s as indicated by the bar (PatchXpress Data). **Right:** GABA concentration-response curves for  $\alpha 3$  (red circles) and  $\alpha 1$  (black squares) (IonWorks Quattro Data).

BACK



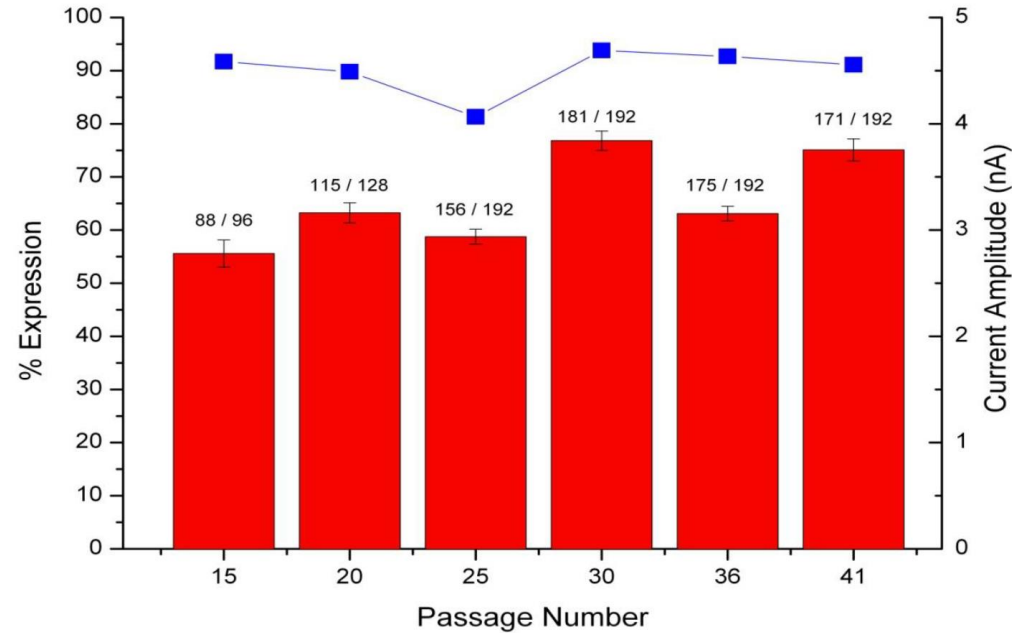
**hGABAA  $\alpha 3/\beta 3/\gamma 2$  Effect of L-838,417 on Currents Evoked by Sub-Maximal GABA evoked responses:** **Left:** The cell was voltage-clamped at a holding potential of -40 mV. Repeated doses of EC<sub>20</sub> GABA (4  $\mu\text{M}$ ) were applied for 5 seconds (black bar). GABA was washed off between doses. The cell was then incubated for 2 minutes in 100 nM L-838,417 followed by co-application of 100 nM L-838,417 (blue bar) and EC<sub>20</sub> GABA (PatchXpress Data). **Right:** Effect of L-838,417 on  $\alpha 1$  and  $\alpha 3$  currents evoked by a sub-maximal (EC<sub>20</sub>) concentration (4  $\mu\text{M}$ ) of GABA (IonWorks Quattro Data).

BACK



**hGABAA  $\alpha 3/\beta 3/\gamma 2$  Effect of Bicuculline on Currents Evoked by 100  $\mu$ M GABA:** **Left:** Inward currents were first evoked by brief (5 s) applications of GABA (black bars) from a holding potential of -40 mV. GABA evoked inward currents in the presence of 100  $\mu$ M bicuculline (red bars) were much reduced in amplitude and readily reversible upon removal of the antagonist. Zero current level is shown by the black dotted line (Manual Patch Clamp Data). **Right:** Typical current traces (upper panel) evoked before (black trace) and after (red trace) the application of 300  $\mu$ M GABA. The zero current level is shown by the black dotted line. Voltage protocol is shown in the lower panel. (IonWorks Quattro Data).

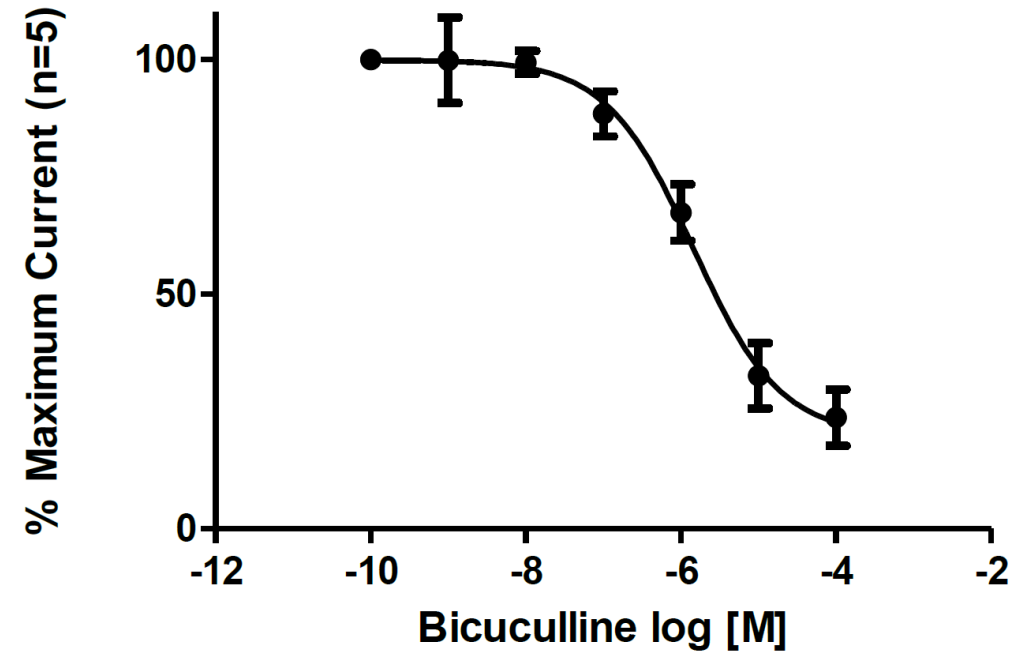
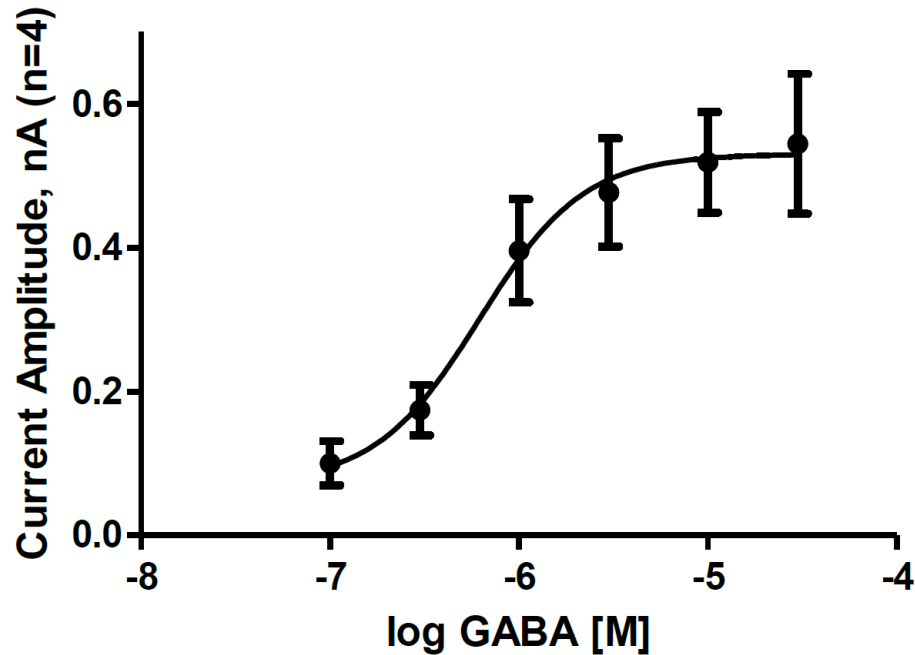
BACK



**hGABAA  $\alpha 3/\beta 3/\gamma 2$  Stability of Expression over Passage:** The blue squares show the percentage of cells expressing a mean peak current >200 pA at 0 mV at cell passages 15, 20, 25, 30, 36 and 41. The corresponding red columns show mean current amplitude (mean  $\pm$  SEM) the number of cells is shown relative to total cell availability (IonWorks Quattro Data).

# hGABAA $\alpha 4/\beta 3/\gamma 2$ (CYL3085)

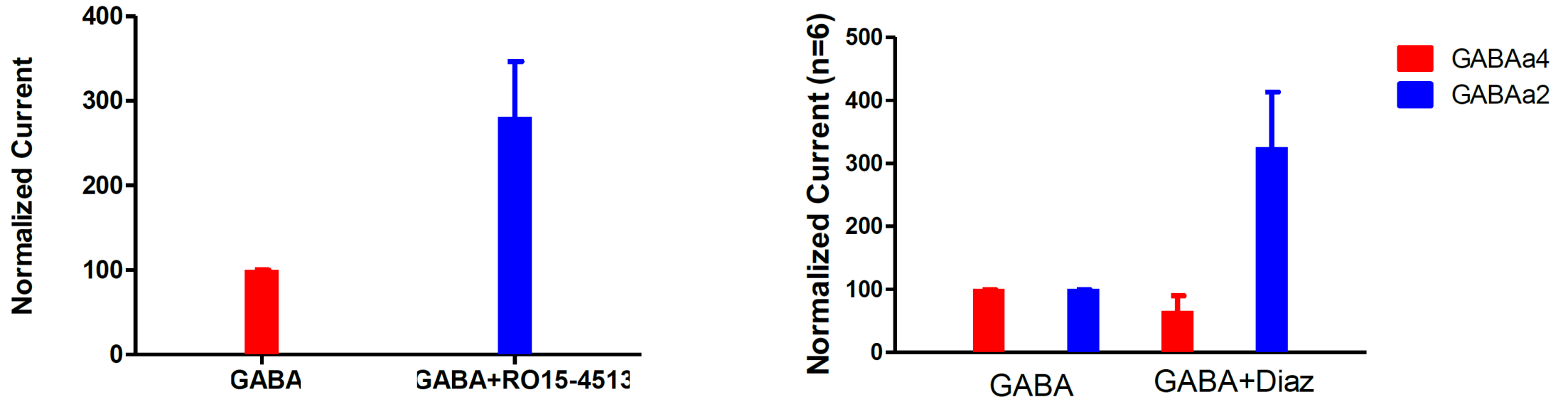
BACK



**hGABAA  $\alpha 4/\beta 3/\gamma 2$  Agonist and Antagonist Dose Response Curves:** **Left:** GABA concentration-response curve at passage 25. Each point indicates the mean ( $\pm$ ) response for 5 cells. We obtained an  $EC_{50}$  of  $0.840 \pm 0.616 \mu M$  and a Hill slope of 1.57. **Right:** Bicuculline inhibition of response to addition of the  $EC_{80}$  concentration of GABA. Each point indicates the response of 5 cells. We obtained an  $IC_{50}$  of  $1.44 \mu M$  and a Hill slope of -0.775 (PatchXpress Data).

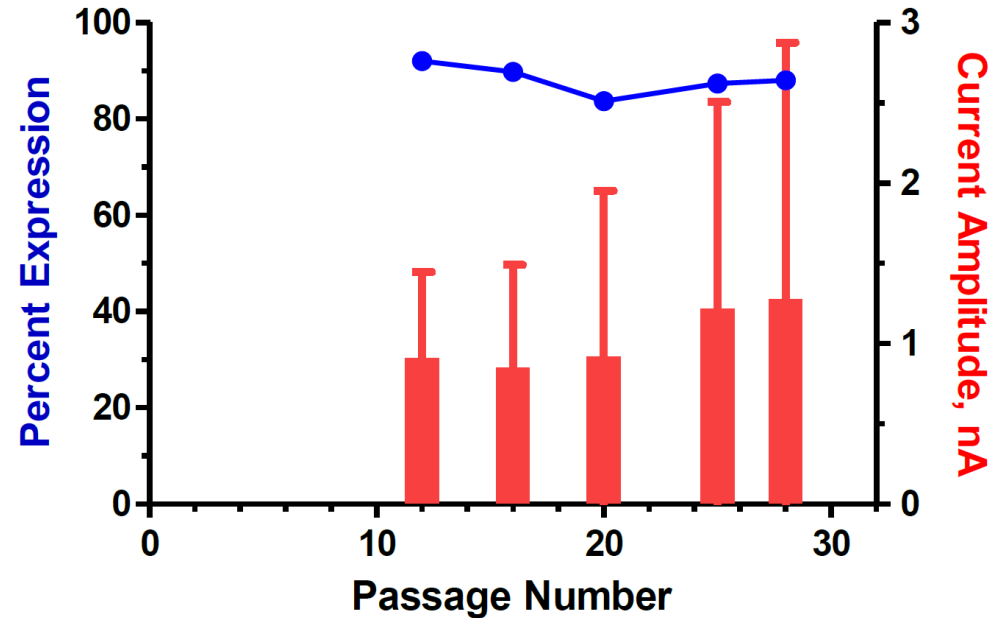


BACK

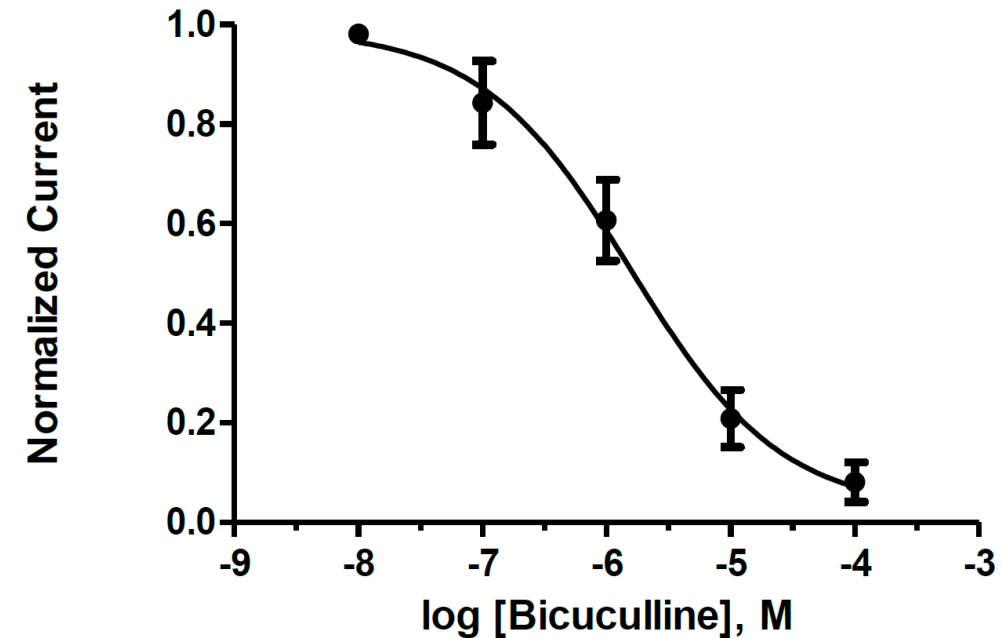
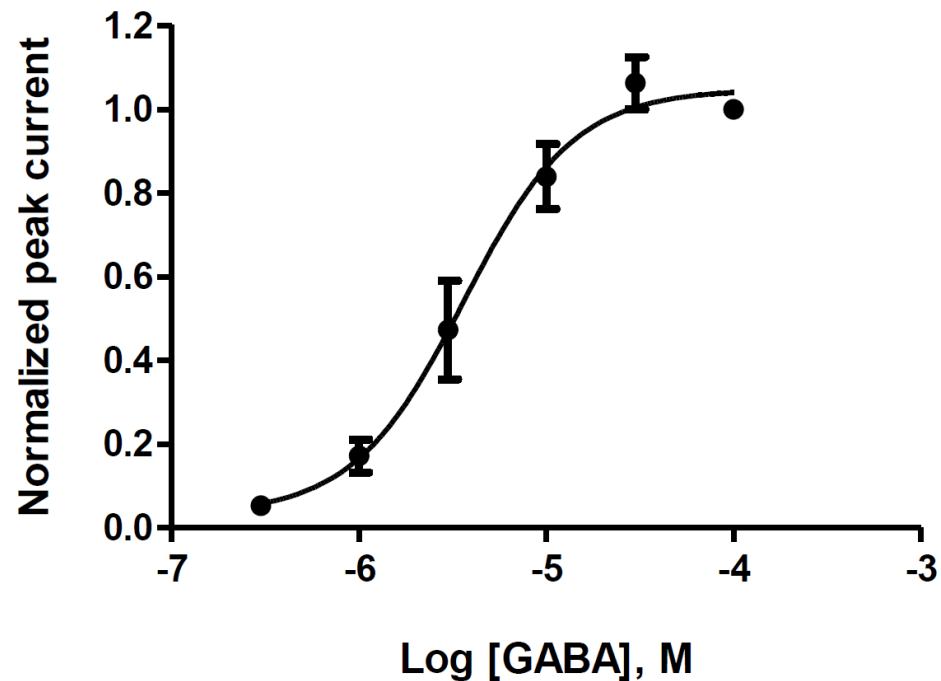


**hGABAA  $\alpha 4/\beta 3/\gamma 2$  Effect of the Benzodiazepine Site Allosteric Modulators on Currents:** **Left:** The positive modifier effect of RO 15-4513 on the hGABAA  $\alpha 4/\beta 2/\gamma 2$  current. Here the hGABAA  $\alpha 4/\beta 2/\gamma 2$  cells were pre-treated with 100 nM of RO 15-4513 followed by an  $EC_{20}$  concentration of GABA + 100 nM RO 15-4513. The GABA induced current was increased approximately 2.5-fold by 100 nM RO 15-4513. **Right:** The effect of 1  $\mu$ M diazepam on the normalized GABA ( $EC_{20}$ ) induced current (n=6 cells; red bars) and the hGABAA  $\alpha 2/\beta 3/\gamma 2$  (n=5; blue bars). 1  $\mu$ M diazepam increased the  $EC_{20}$  GABA-induced current in the hGABAA  $\alpha 2/\beta 3/\gamma 2$  cells, but did not show a positive modulating effect on the hGABAA  $\alpha 4/\beta 3/\gamma 2$  current. (PatchXpress Data). **Reference:** Knoflach F et al. (1996). Pharmacological modulation of the diazepam-insensitive recombinant  $\gamma$ -aminobutyric acidA receptors  $\alpha 4\beta 2\gamma 2$  and  $\alpha 6\beta 2\gamma 2$ . *Molecular Pharmacology*, 50:1253-1261.

BACK

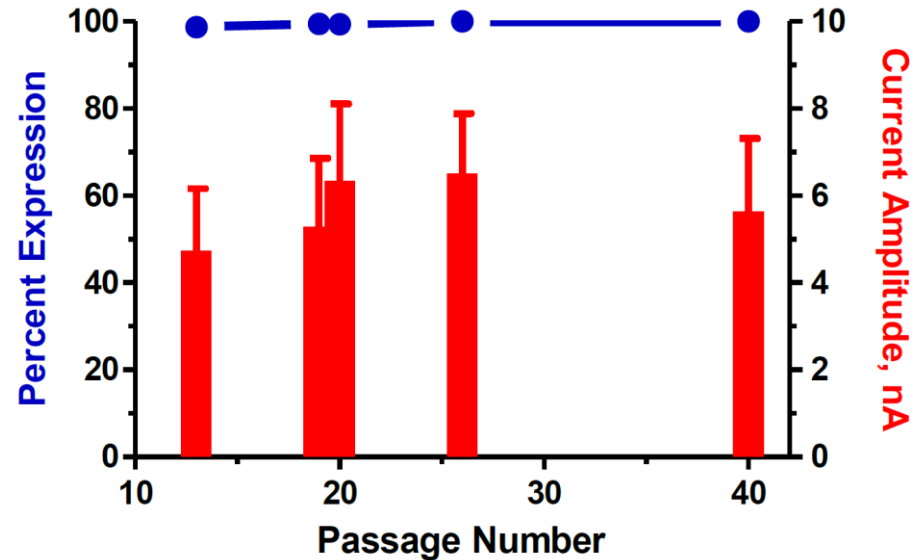
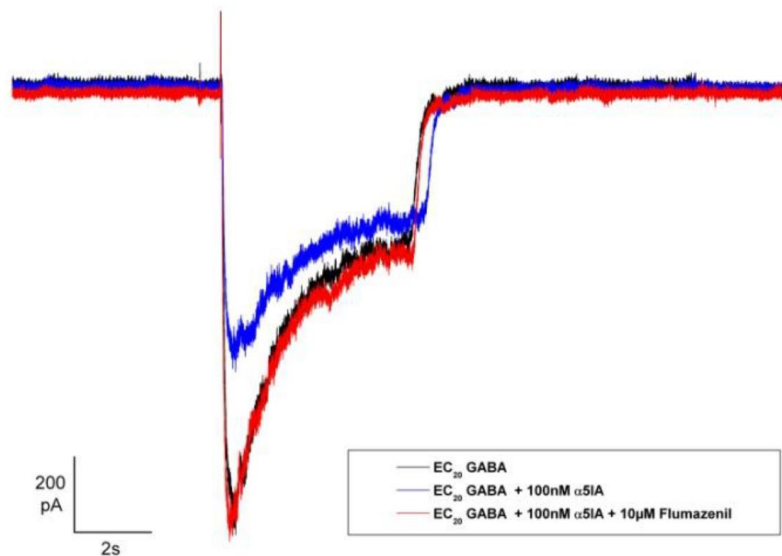


**hGABAA  $\alpha 4/\beta 3/\gamma 2$  Stability of Expression over Passage:** The blue line shows the percentage of cells expressing a mean peak inward current  $>0.25$  nA at  $-40$  mV at cell passages 11, 15, 20, 25 and 28. The red bars show the mean current amplitude (mean  $\pm$  SD) for 73-330 cells per experiment. (IonWorks HT Data).

[BACK](#)

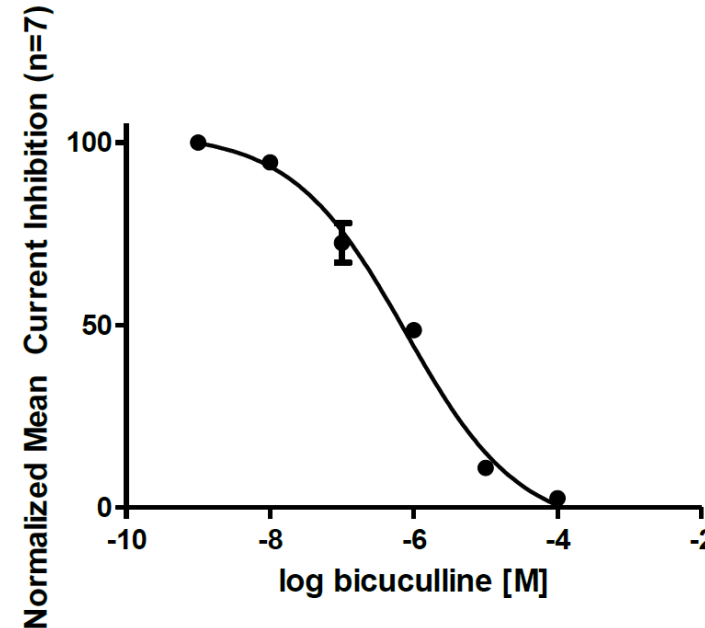
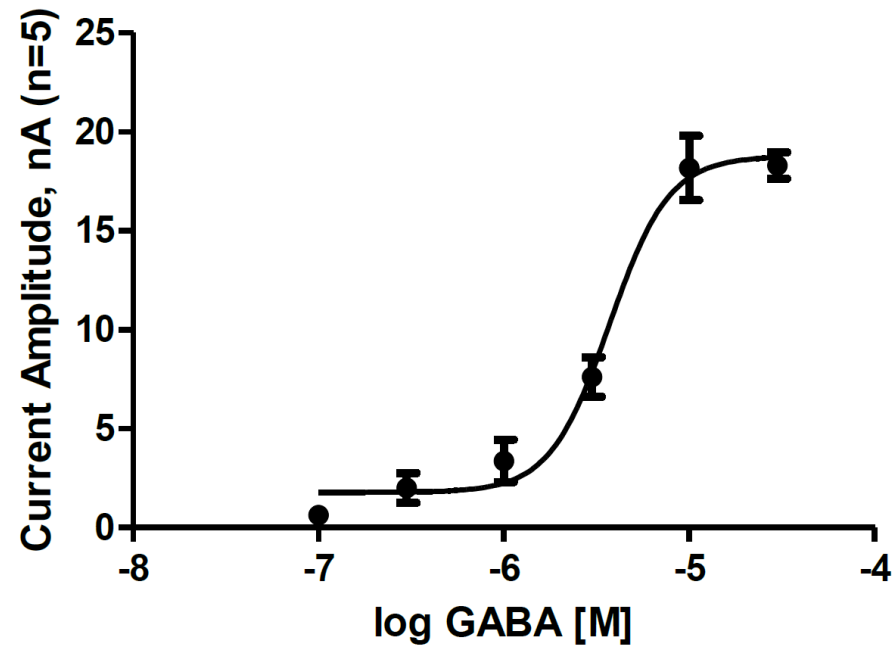
**hGABAA  $\alpha 5/\beta 3/\gamma 2$  Agonist and Antagonist Dose Response Curves:** **Left:** GABA concentration-response curve. Each point indicates the mean ( $\pm$ SEM) response for 3 cells. We obtained an  $EC_{50}$  of 3.6  $\mu$ M and a Hill slope of 1.0. **Right:** Bicuculline inhibition of response to addition of 100  $\mu$ M GABA. Each point indicates the mean ( $\pm$ SEM) response of 3 cells. We obtained an  $IC_{50}$  of 1.6  $\mu$ M and a Hill slope of -0.72 (PatchXpress Data).

BACK



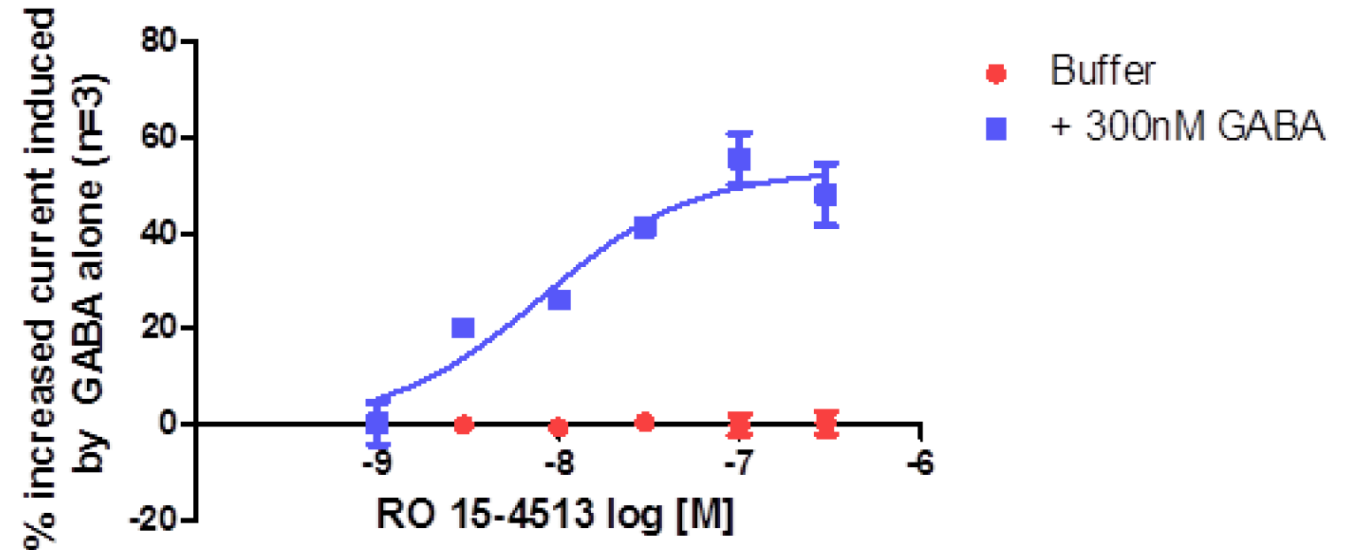
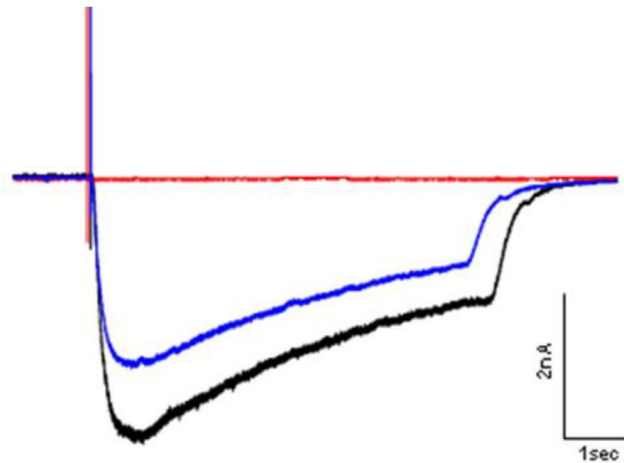
**hGABAA  $\alpha 5/\beta 3/\gamma 2$  Effect of  $\alpha 5$ IA, Stability of Expression over Passage:** **Left:** The black trace shows the response to addition of an EC<sub>20</sub> of GABA. After washout, 100 nM  $\alpha 5$ IA was added alone and had no effect (not shown). After a 2 min incubation with 100 nM  $\alpha 5$ IA, the response to addition of an EC<sub>20</sub> of GABA (blue trace) was now inhibited. In five cells, 100 nM  $\alpha 5$ IA reduced the EC<sub>20</sub> GABA current to 60.9  $\pm$  8.5% of control. Following washout, the response to the EC<sub>20</sub> of GABA completely recovered (red trace). The effect of 100 nM  $\alpha 5$ IA was completely blocked by 10  $\mu$ M flumazenil, indicating the effect is mediated through the benzodiazepine binding site on the GABA A  $\alpha 5/\beta 3/\gamma 2$  receptor (PatchXpress Data). **Right:** The blue line shows the percentage of cells expressing a mean peak inward current >0.5 nA at -40 mV at cell passages 13, 19, 20, 26 and 40. The red bars show the mean current amplitude (mean  $\pm$  SD) for 73-351 cells per experiment (IonWorks HT Data).

BACK



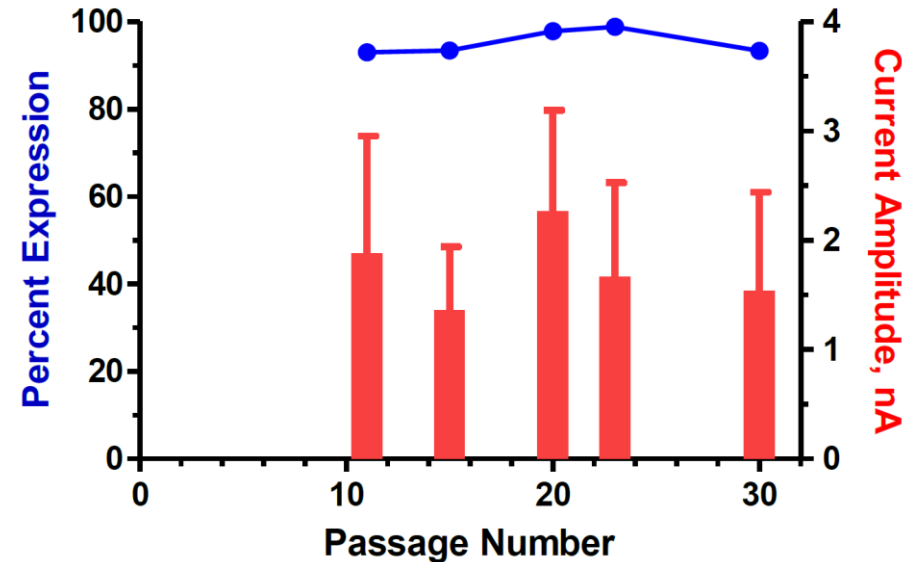
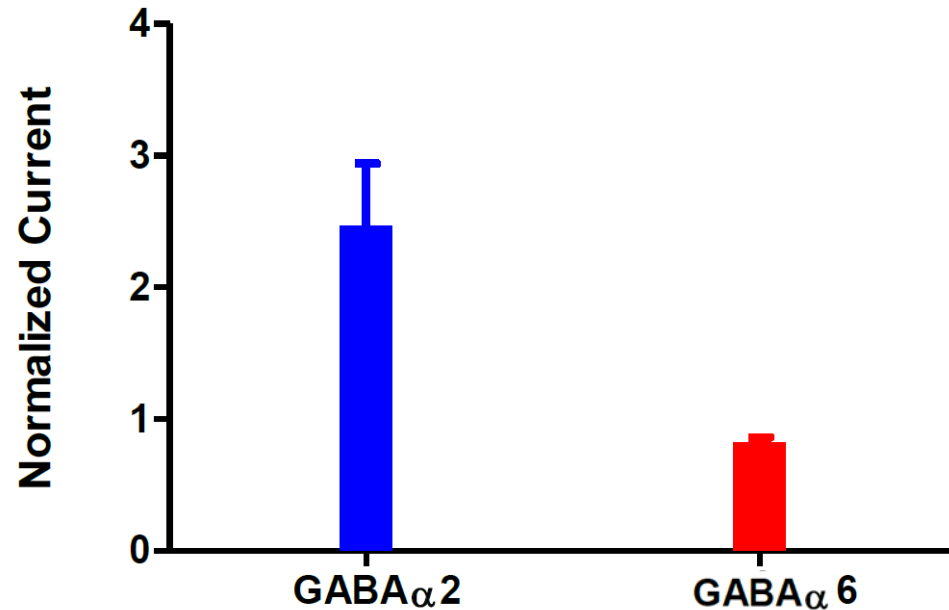
**hGABAA  $\alpha 6/\beta 3/\gamma 2$  Agonist and Antagonist Dose Response Curves:** **Left:** hGABAA  $\alpha 6/\beta 3/\gamma 2$ -HEK cells at passage 15 were treated with increasing concentrations of GABA and the response measured. Each point indicates the mean ( $\pm$ SD) response for 5 cells. We obtained an  $EC_{50}$  of 3.72  $\mu$ M and a Hill slope of 2.71 **Right:** The block by bicuculline of the  $EC_{80}$  GABA induced current was measured. Each point indicates the response of 7 cells. We obtained an  $IC_{50}$  of 0.823  $\mu$ M and a Hill slope of -0.55. (PatchXpress Data).

BACK



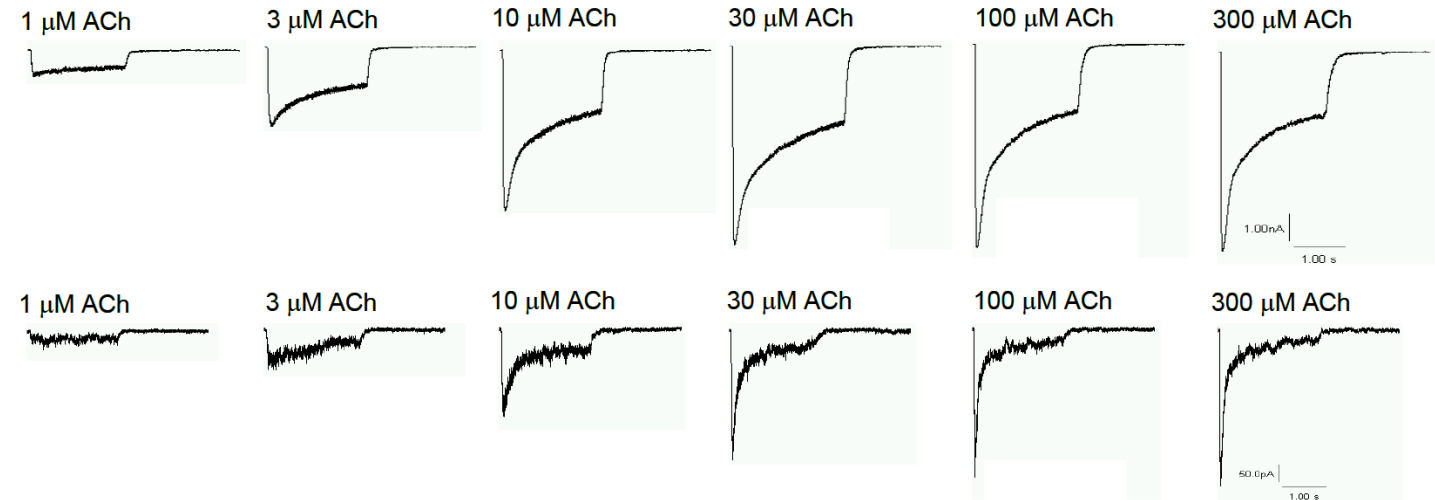
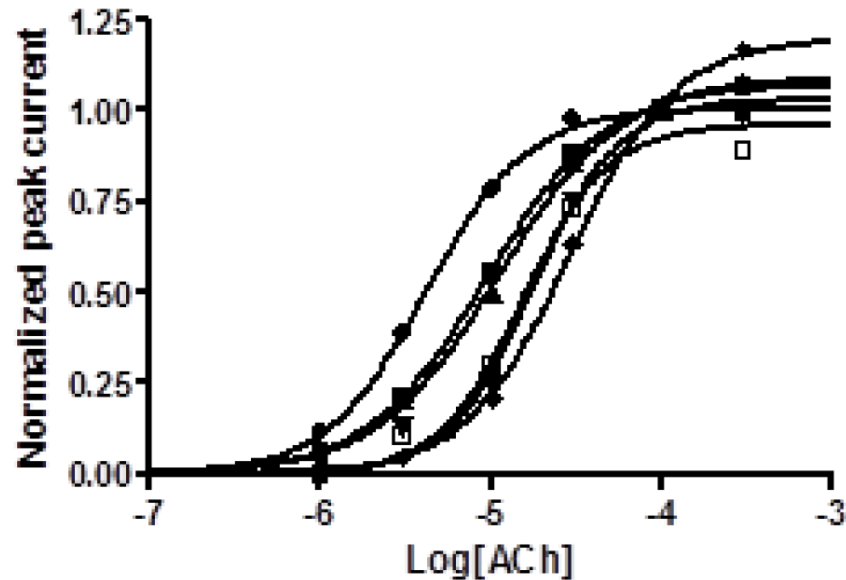
**hGABAA  $\alpha 6/\beta 3/\gamma 2$  Effect of the Benzodiazepine Site Allosteric Modulators on Currents:** **Left:** The positive modifier effect of RO 15-4513 on currents. Cells treated with the  $EC_{20}$  concentration of GABA (blue trace). After washout, 0.3  $\mu M$  RO 15-4513 was added alone and had no effect (red trace). After a 2 min incubation with 0.3  $\mu M$  RO 15-4513, the response to the addition of an  $EC_{20}$  concentration of GABA+RO 15-4513 (black trace) was enhanced. **Right:** Concentration-dependent enhancement in the GABA ( $EC_{20}$ ) induced current by RO 15-4513. The normalized GABA-induced current was increased approximately 60% by the highest concentrations of RO 15-4513. The  $EC_{50}$  for RO 15-4513 was 8.12 nM and the Hill slope of the curve was 1.04. A second partial agonist modifier, bretazenil, also increased the GABA-induced current at a concentration of 100  $\mu M$  (data not shown). (PatchXpress Data). **References:** Knoflach F et al. (1996). Pharmacological modulation of the diazepam-insensitive recombinant  $\gamma$ -aminobutyric acidA receptors  $\alpha 4\beta 2\gamma 2$  and  $\alpha 6\beta 2\gamma 2$ . *Molecular Pharmacology*, 50:1253-1261. Hadingham KL et. al.(1996) Cloning of cDNAs encoding the human  $\gamma$ -aminobutyric acid Type A receptor  $\alpha 6$  subunit and characterization of the pharmacology of  $\alpha 6$  containing receptors. *Molecular Pharmacology* 49: 253-259.

BACK



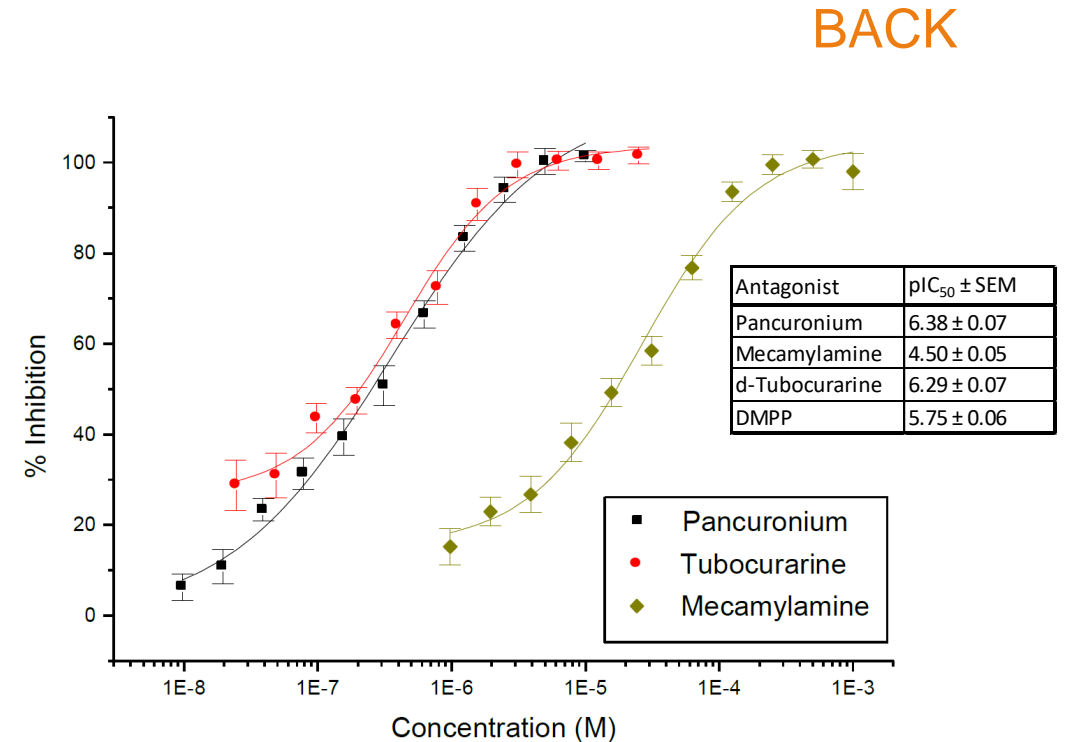
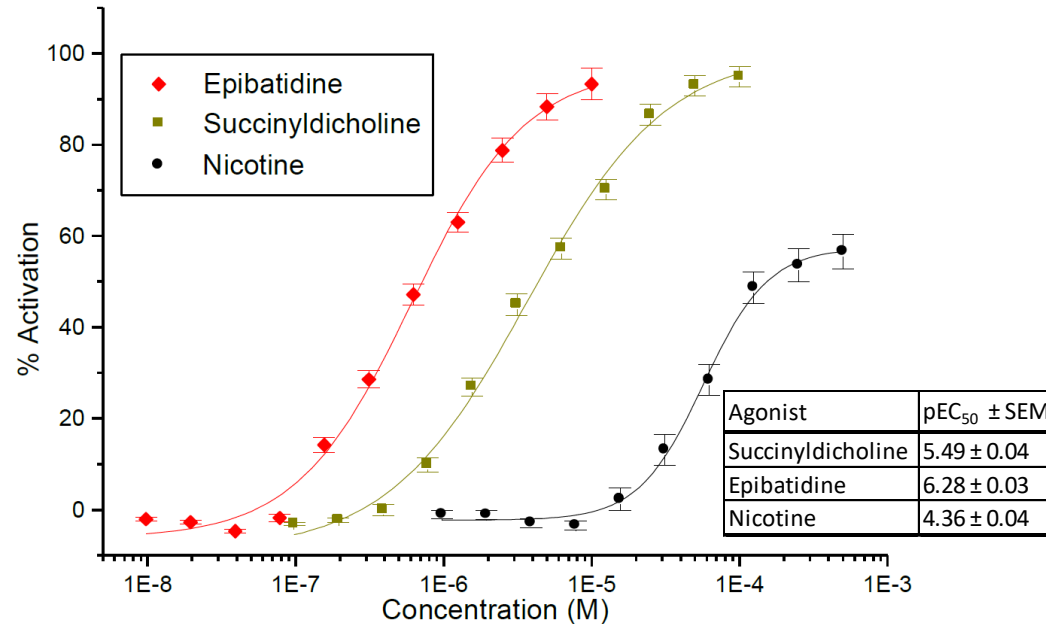
**The benzodiazepine site allosteric modulator diazepam does not modulate the hGABAA  $\alpha 6/\beta 3/\gamma 2$  current, Stability of Expression over Passage:** Left: we compared the effect of 10  $\mu\text{M}$  diazepam on the GABA (EC<sub>20</sub>) induced current in HEK cells expressing either the hGABAA  $\alpha 2/\beta 3/\gamma 2$  current (n=7 cells) or on the hGABAA  $\alpha 6/\beta 3/\gamma 2$  current (n=5 cells). Diazepam increased the EC<sub>20</sub> GABA-induced current in the hGABAA  $\alpha 2/\beta 3/\gamma 2$  cells (blue bar) approximately 2.5 fold over the normalized current, but did not show a positive modifier effect on the hGABAA  $\alpha 6/\beta 3/\gamma 2$  current (red bar). (PatchXpress Data) **Right:** The blue line shows the percentage of cells expressing a mean peak inward current >0.25 nA at -40 mV at cell passages 11, 15, 20, 23 and 30. The red bars show the mean current amplitude (mean  $\pm$  SD) for 67-169 cells per experiment. (IonWorks Quattro Data). **References:** Knoflach F et al. (1996). Pharmacological modulation of the diazepam-insensitive recombinant  $\gamma$ -aminobutyric acidA receptors  $\alpha 4\beta 2\gamma 2$  and  $\alpha 6\beta 2\gamma 2$ . *Molecular Pharmacology*, 50:1253-1261. Hadingham KL et. al.(1996) Cloning of cDNAs encoding the human  $\gamma$ -aminobutyric acid Type A receptor  $\alpha 6$  subunit and characterization of the pharmacology of  $\alpha 6$  containing receptors. *Molecular Pharmacology* 49: 253-259.

BACK



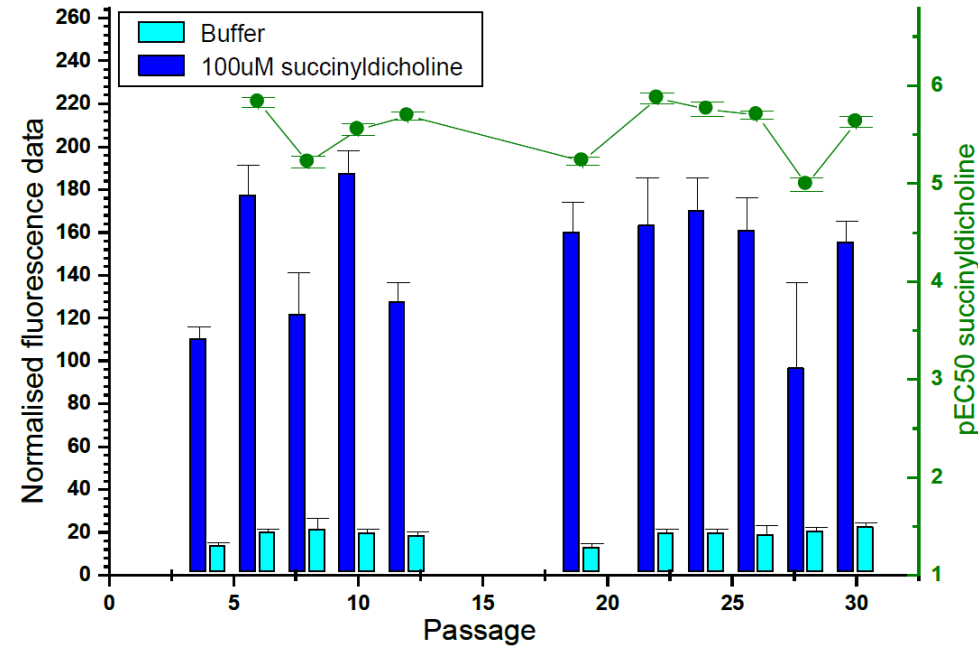
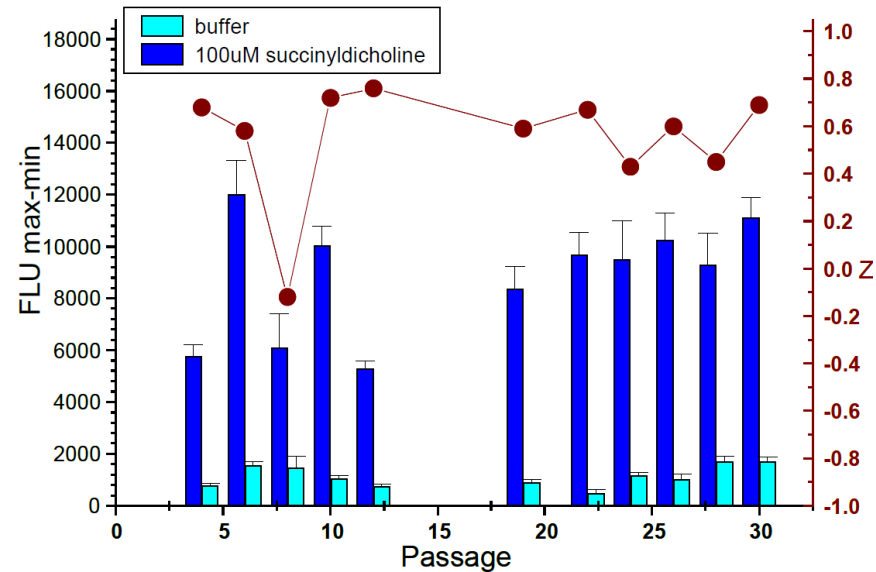
**Concentration-Response Curves and Representative Current Records for Activation of hnAChR  $\alpha 1/\beta 1/\delta/\epsilon$  currents:** **Left:** Concentration-response curves for ACh-evoked currents. The abscissa shows the log concentration of ACh (M) and the ordinate the peak current amplitude normalized to the 100  $\mu$ M evoked current amplitude value. Each point represents the single value from each tested cells (6 cells tested). From the 3 parameter logistic equation the  $pEC_{50}$  values range from 5.4 to 4.5 (mean  $\pm$  SEM =  $4.92 \pm 0.12$ ). **Right:** ACh-induced currents recorded from two different cells, activation was by increasing concentrations of agonist applied for 2 s every 1 minute. The cells are representative of the different degrees of desensitization that was observed during the experiments. (Manual Patch Clamp Data).





**hnAChR  $\alpha 1/\beta 1/\delta/\epsilon$  Agonist and Antagonist Dose Response Curves:** Left: To assess agonist pharmacology, three agonists were tested. pEC<sub>50</sub> values are shown in the inset Table Right: Representative antagonist dose response curves (median ± SEM) (FLIPR Calcium Assay Data).

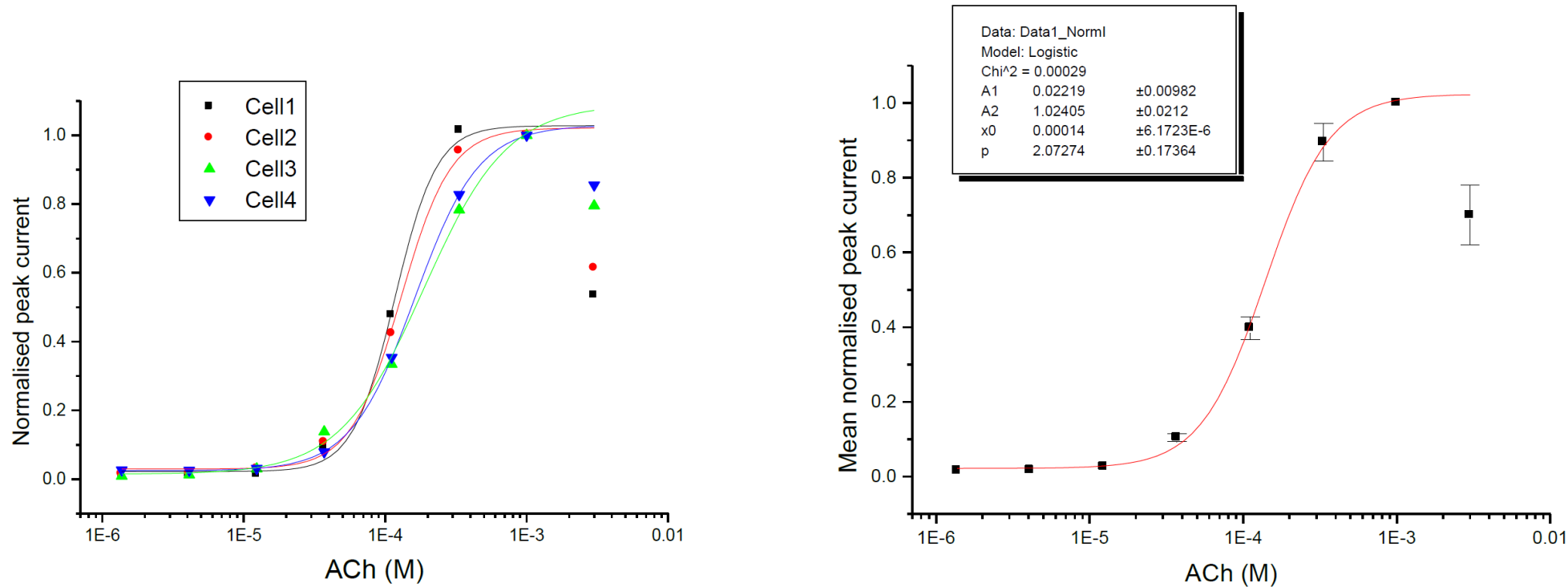
BACK



**hnAChR  $\alpha 1/\beta 1/\delta/\epsilon$  Stability of the FLIPR fluorescence Assay Over Cell Passage:** **Left:** The FLIPR fluorescence signal and Z-prime over cell passage. The fluorescence signal window calculated for each well was the post-compound response minus the basal fluorescence for that well (n=16). **Right:** Stability of the FLIPR normalized fluorescence signal and succinylcholine pEC50 over cell passage (FLIPR Calcium Assay Data).

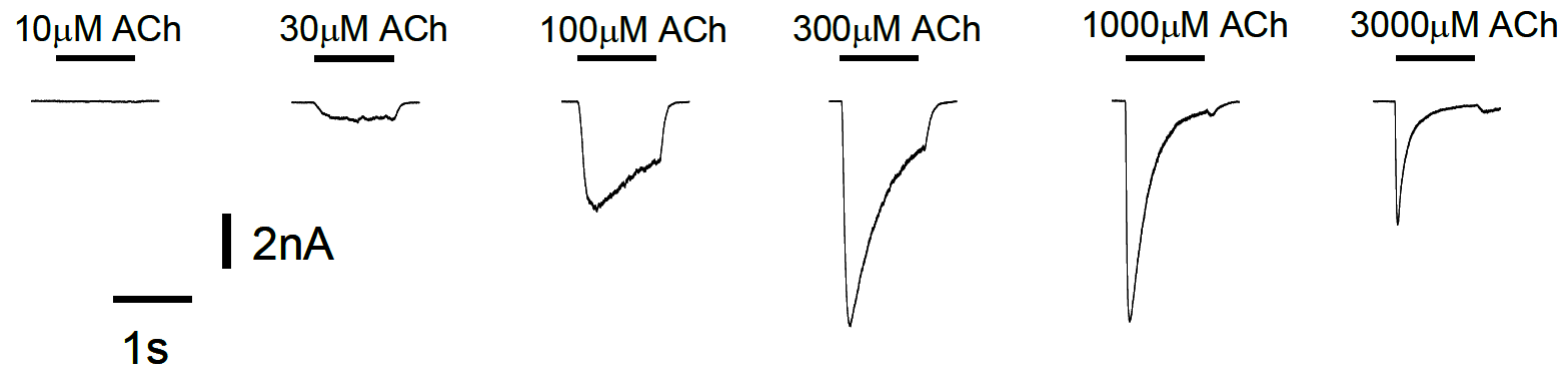
# nAChR $\alpha 3/\beta 4$ (CYL3057)

BACK



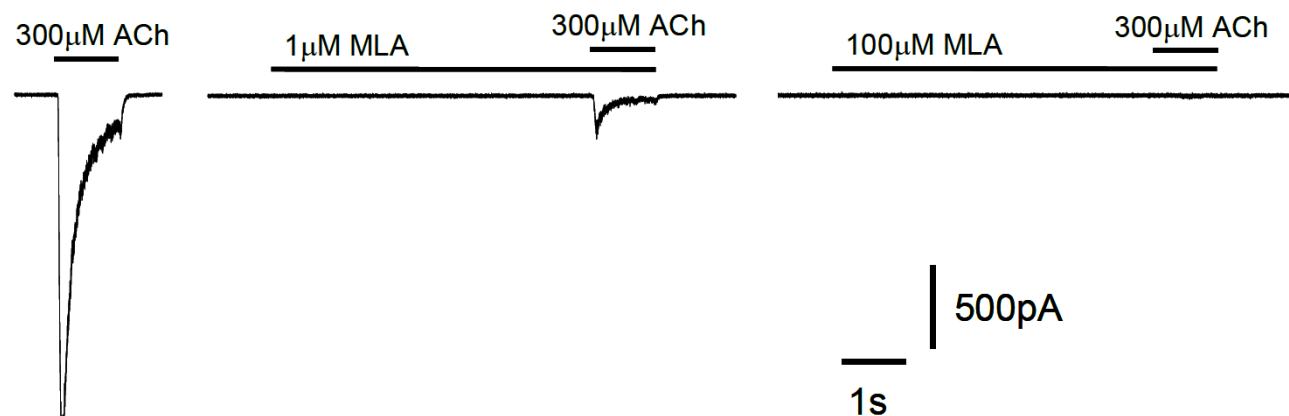
**hnAChR  $\alpha 3/\beta 4$  Agonist Activation:** **Left:** Concentration-response curves for ACh-evoked currents. The x-axis shows the log concentration of ACh (M) and the y-axis the peak current amplitude normalized to the 1 mM evoked current amplitude value. Each point represents the single value from each tested cell (4 cells tested). **Right:** Mean data. EC<sub>50</sub> value = 140 ± 6.2  $\mu$ M (mean ± SEM, n=4) (Manual Patch Clamp Data).

BACK

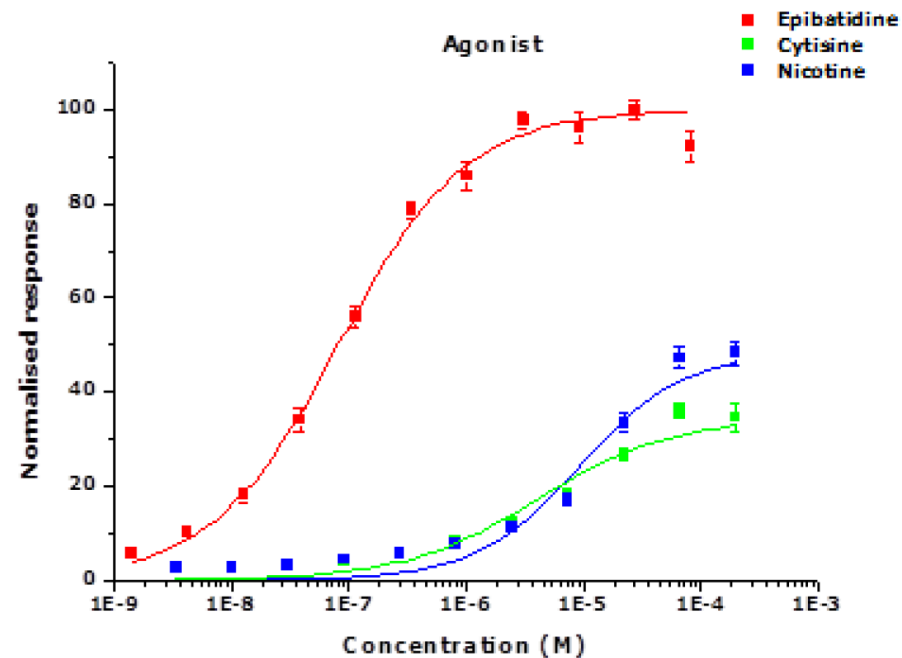


**hnAChR  $\alpha3/\beta4$  Raw Data Currents:** ACh-induced currents recorded from a typical cell. Activation was by increasing concentrations of agonist (10-3000  $\mu\text{M}$ ) applied for 1 s. This cell was representative of the degree of desensitization that was observed at concentrations of ACh >1 mM during experiments. (Manual Patch Clamp Data).

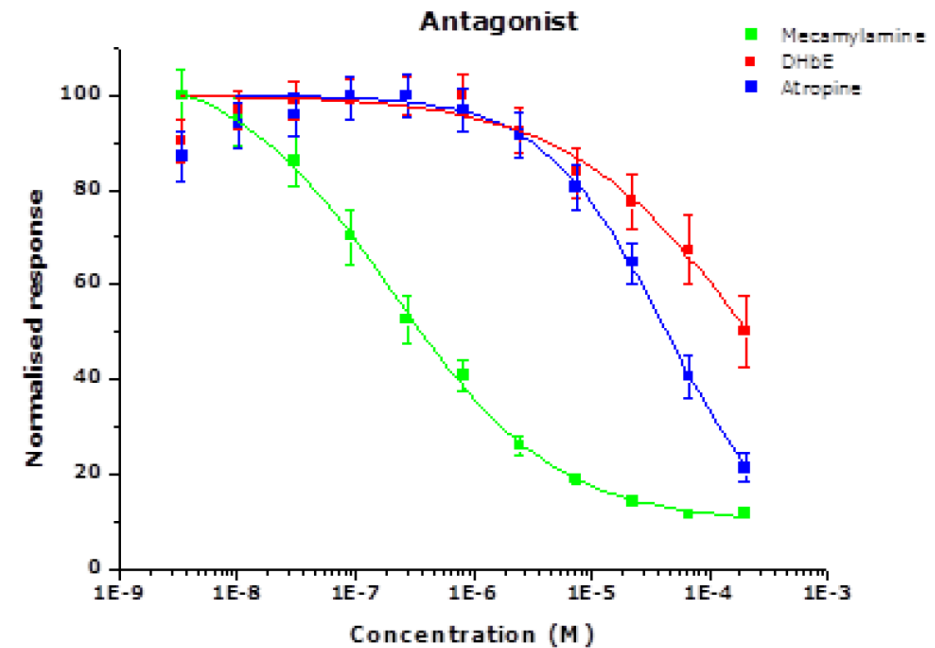
BACK



**hnAChR  $\alpha 3/\beta 4$  Methyllycaconitine (MLA) Pharmacology:** The nAChR  $\alpha 3/\beta 4$  current elicited by 300  $\mu\text{M}$  ACh was completely blocked by 100  $\mu\text{M}$  MLA and to a lesser degree by 1  $\mu\text{M}$  MLA. Following a pre-application of 300  $\mu\text{M}$  ACh, cells were perfused with MLA (1  $\mu\text{M}$  or 100  $\mu\text{M}$ ) for 5 s followed by a 1 s co-application of 300  $\mu\text{M}$  ACh. (Manual Patch Clamp Data).



Agonist	hnAChR $\alpha3/\beta4$ -HEK293 EC <sub>50</sub> $\pm$ SEM
Epibatidine	81.4 $\pm$ 7.39 nM
Nicotine	9.16 $\pm$ 1.77 $\mu$ M
Cytisine	4.16 $\pm$ 0.94 $\mu$ M

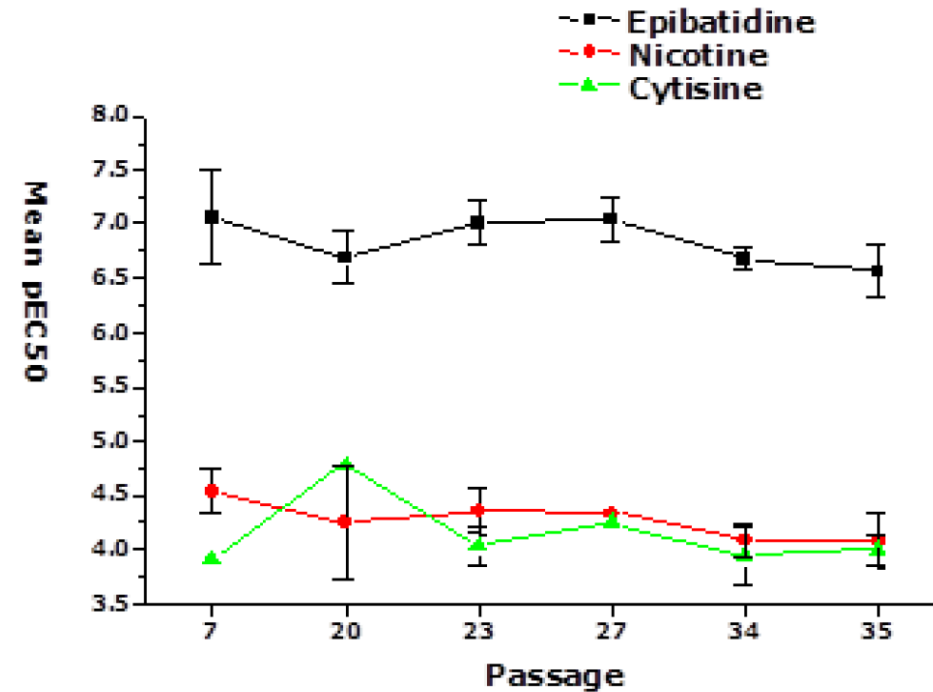
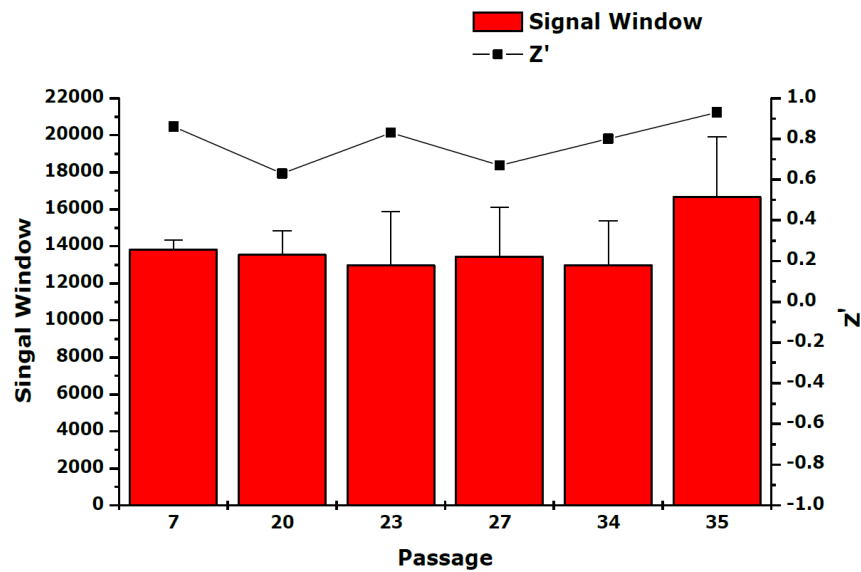


Antagonist	hnAChR $\alpha3/\beta4$ -HEK293 IC <sub>50</sub> $\pm$ SEM
Mecamylamine	481 $\pm$ 83.6 nM
DHbE	210 $\pm$ 50.0 $\mu$ M
Atropine	40.0 $\pm$ 6.22 $\mu$ M

BACK

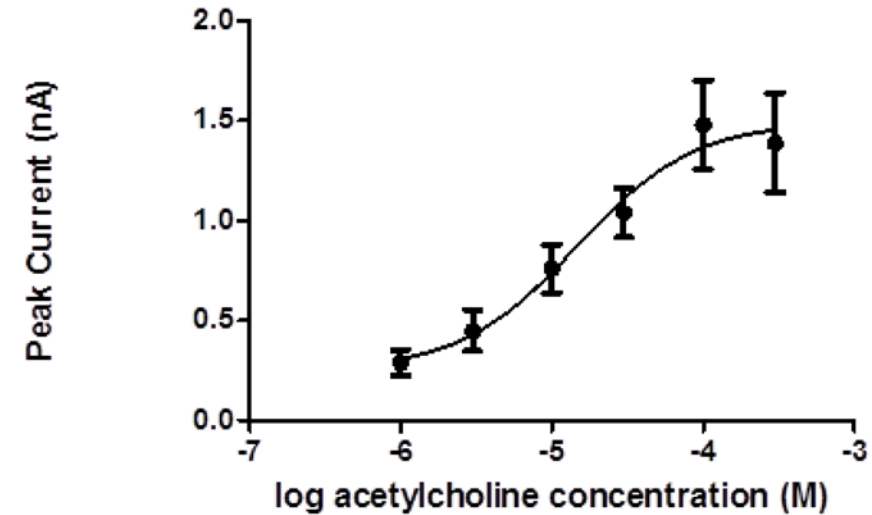
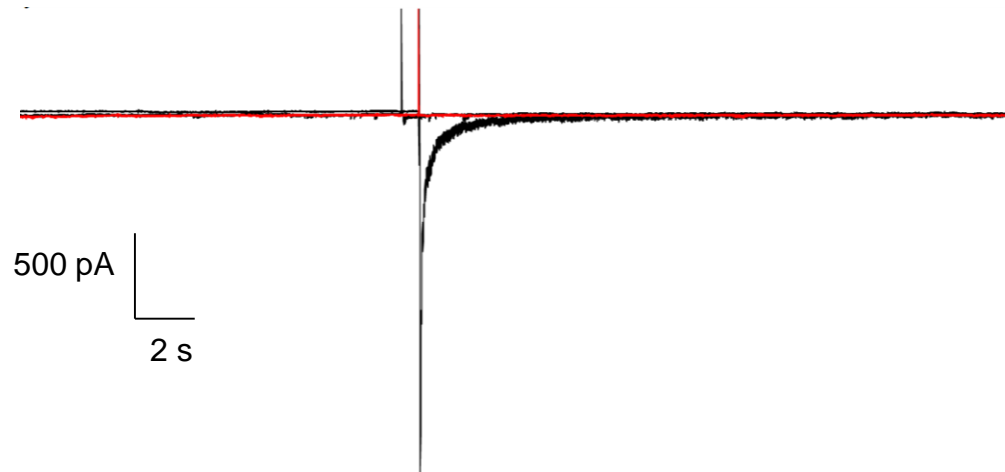
**hnAChR  $\alpha3/\beta4$  Agonist and Antagonist Fluorescent Calcium Assay:** **Left:** To assess agonist pharmacology, three compounds were tested (Figure 3). EC<sub>50</sub> values are shown in the Table. The values obtained are in close agreement with published data for [Ca<sup>2+</sup>]<sub>i</sub> flux experiments (Stauderman et al., 1998). **Right:** To assess antagonist pharmacology, the ability of three compounds to block the epibatidine response at its EC<sub>80</sub> concentration on the day of assay (6-10  $\mu$ M) was tested (Figure 4). IC<sub>50</sub> values for the block of the epibatidine response are shown in the Table. (FLIPR Calcium Assay Data).

BACK



**hnAChR  $\alpha 3/\beta 4$  Stability of Fluorescent Calcium Assay over Cell Passages:** **Left:** Stability of the FLIPR fluorescence signal and Z-prime over passage. The fluorescence signal window calculated for each well was the post-compound response minus the basal fluorescence for that well. **Right:** Stability of agonist pEC<sub>50</sub> values over passage. (FLIPR Calcium Assay Data).

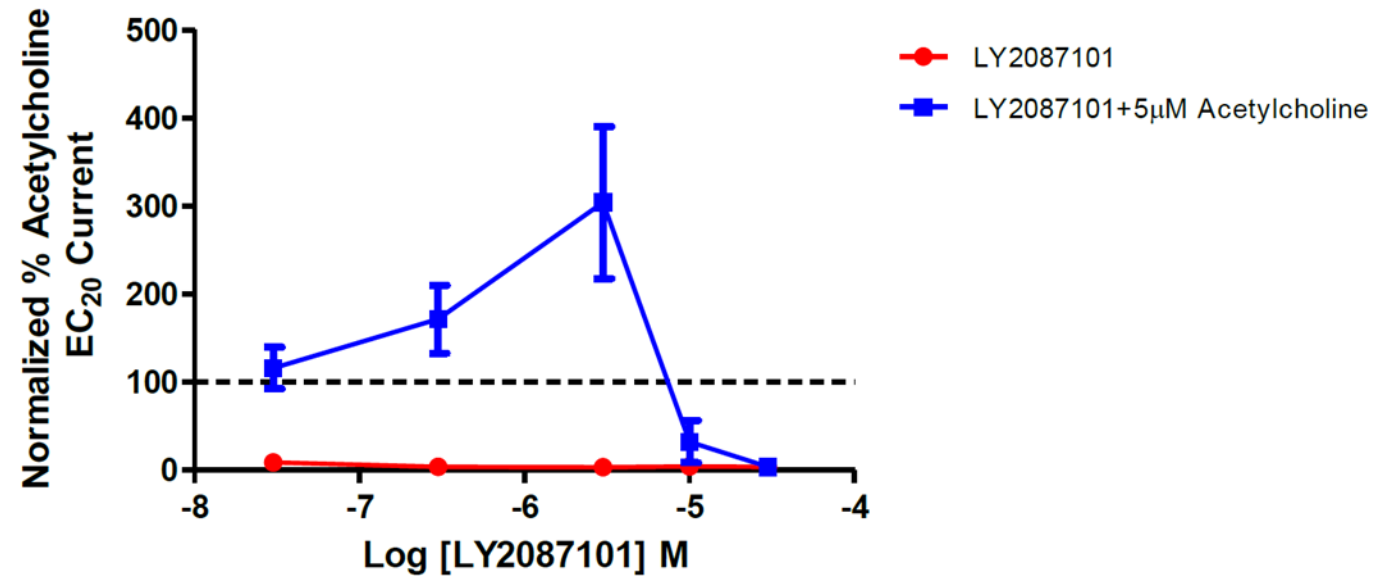
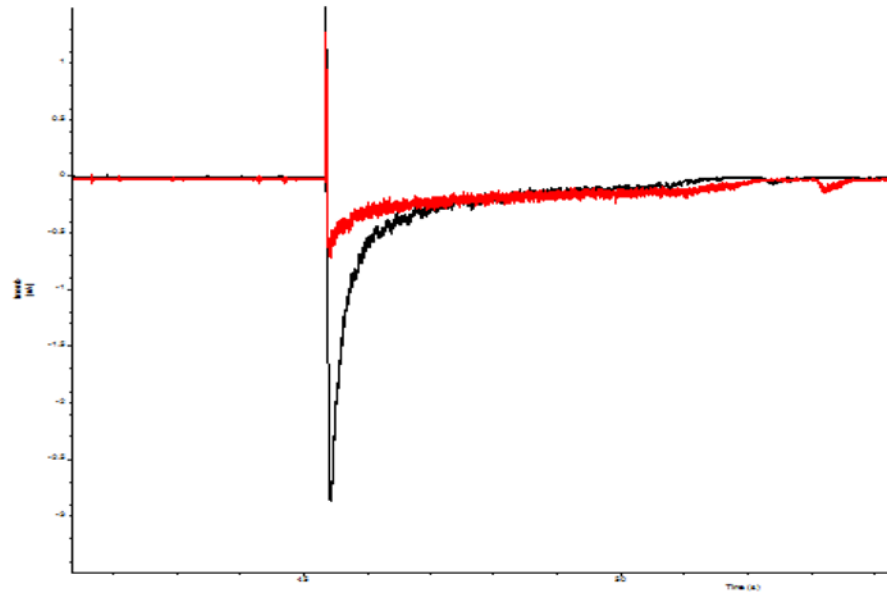
BACK



**hnAChR  $\alpha 4/\beta 2$  Agonist Activation:** **Left:** The black trace shows approximately 2 nA of current induced by the application of 100  $\mu$ M acetylcholine. The red trace shows the same cell after washout of the acetylcholine followed by a 3 minute preincubation with 20  $\mu$ M mecamylamine and then stimulation of the current by the co-application of 20  $\mu$ M mecamylamine + 100  $\mu$ M acetylcholine. Treatment of the cell with mecamylamine blocked the current elicited by the application of acetylcholine (PatchXpress Data). **Right:** The addition of acetylcholine elicits an inward current in a concentration-dependent manner. Peak inward current was approximately 1.5 nA and we found an  $EC_{50}$  of 14.7  $\mu$ M with a Hill slope coefficient of 1.12 (PatchXpress Data).

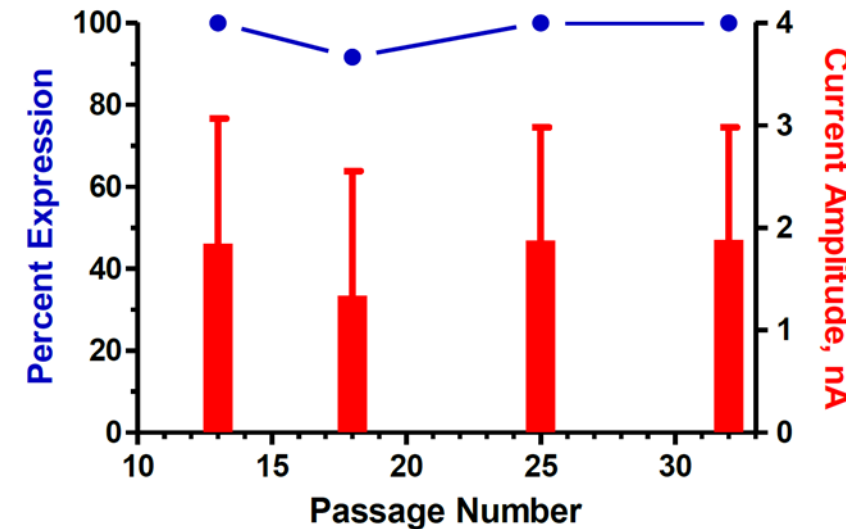
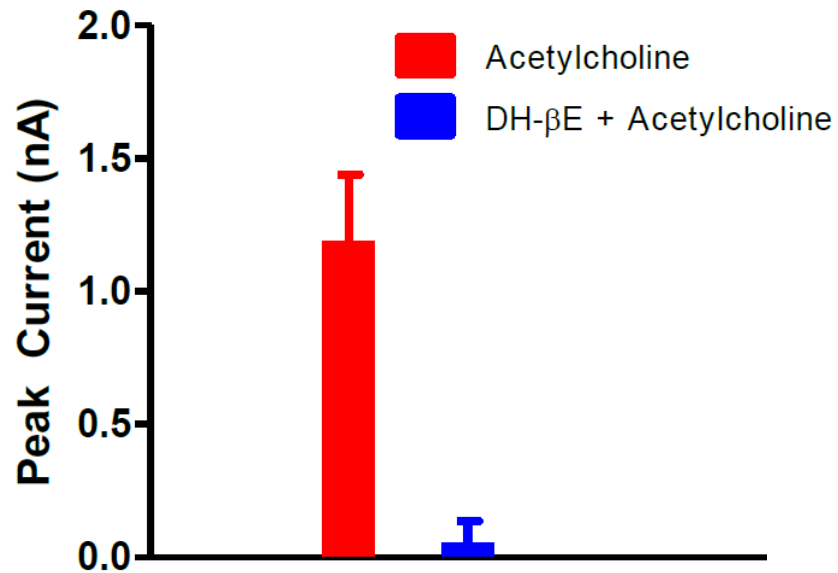


BACK



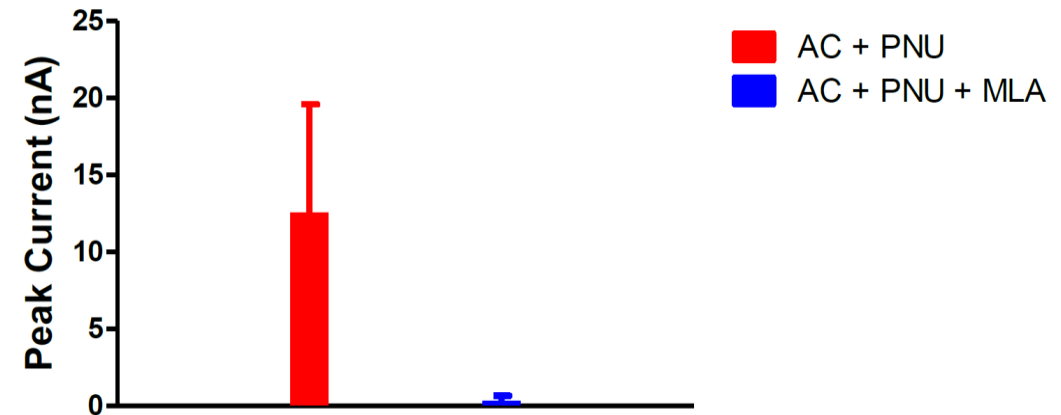
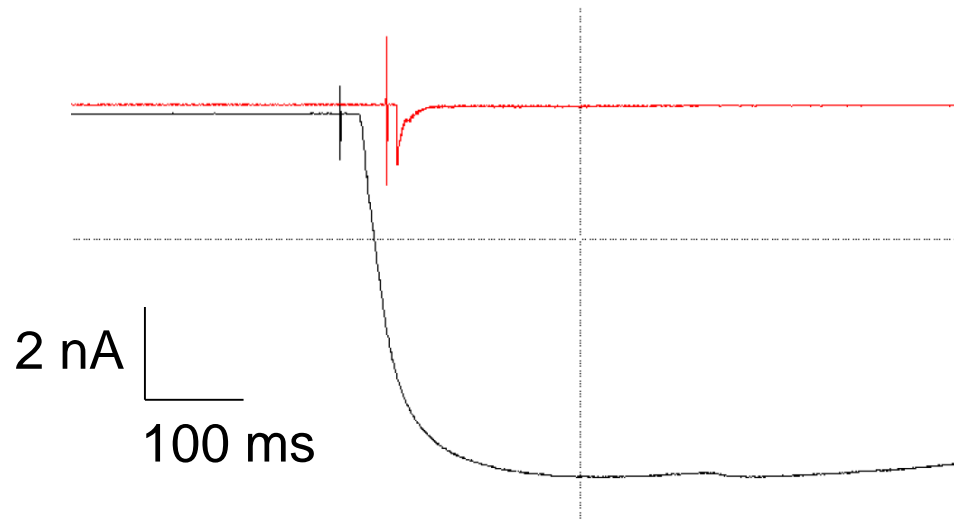
**hnAChR  $\alpha 4/\beta 2$  Positive Allosteric Modulation of the Acetylcholine Elicited Current:** **Left:** The red trace represents the current elicited by the addition of 5  $\mu$ M acetylcholine. Following washout and a three minute incubation with 3  $\mu$ M LY2087171, the black trace shows the current that results from the addition of 5  $\mu$ M acetylcholine + 3  $\mu$ M LY2087101. In this cell the addition of LY2087101 positively modulated the acetylcholine-induced current approximately three fold (PatchXpress Data). **Right:** Currents induced by the approximate EC<sub>20</sub> concentration of acetylcholine (5  $\mu$ M) are represented by the dotted line at 100% on the Y-axis. Pre-incubation of the cells with increasing amounts of LY2087101 (6) for three minutes (red line) followed by the addition of 5  $\mu$ M acetylcholine + LY2087101 (blue line) resulted in the positive modulation of the current induced by acetylcholine in a concentration-dependent manner. At 10 and 30  $\mu$ M LY2087101 inhibited the current elicited by acetylcholine (PatchXpress Data).

BACK



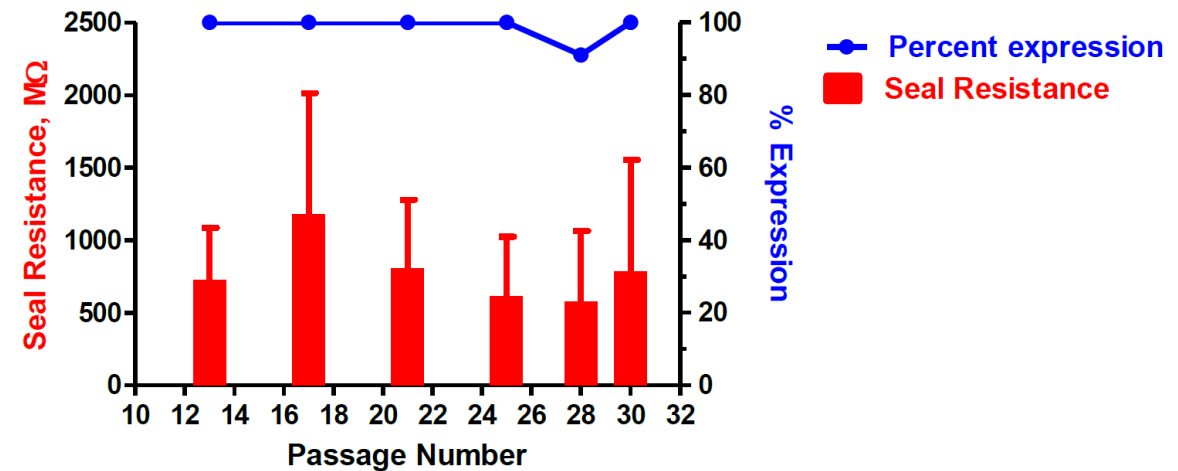
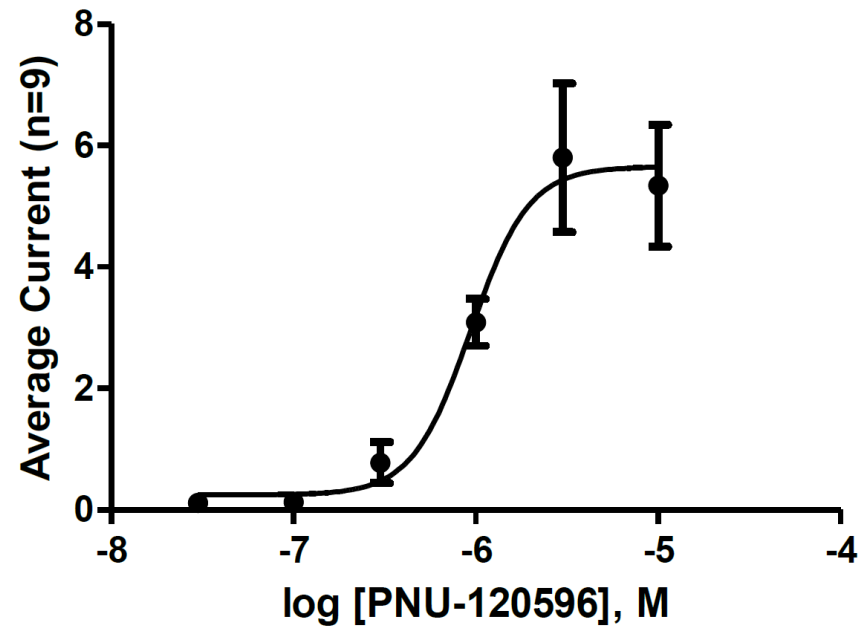
**hnAChR  $\alpha 4/\beta 2$  Block of Acetylcholine Induced Current by Dihydro-β-erythroidine, Stability of Expression over Passage:** **Left:** The red bar represents the current elicited by 100 μM acetylcholine. Following washout and a four minute preincubation with 10 μM dihydro-β-erythroidine (DH-βE), the inhibition of the current induced by the addition of 100 μM acetylcholine in the presence of 10 μM DH-βE is represented by the blue bar. These data are in agreement with previously published data (PatchXpress Data). **Right:** The stability of expression was determined on the PatchXpress® by the addition of 100 μM acetylcholine at a holding potential of -60 mV. The blue line shows the percentage of cells expressing a mean peak inward current >500 pA at cell passages 13, 18, 25 and 32. The red bars show the mean peak current amplitude (mean ± SD) for 7-14 cells per experiment. Functional expression of the hnAChR  $\alpha 4/\beta 2$  currents was > 91% through 32 passages and the mean current amplitude was > 1.33 nA. (PatchXpress Data).

BACK



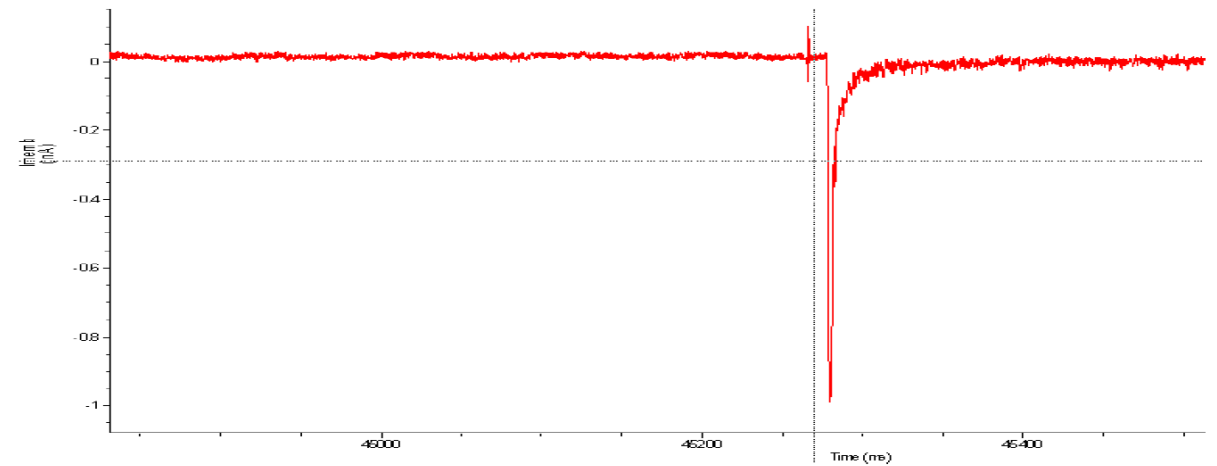
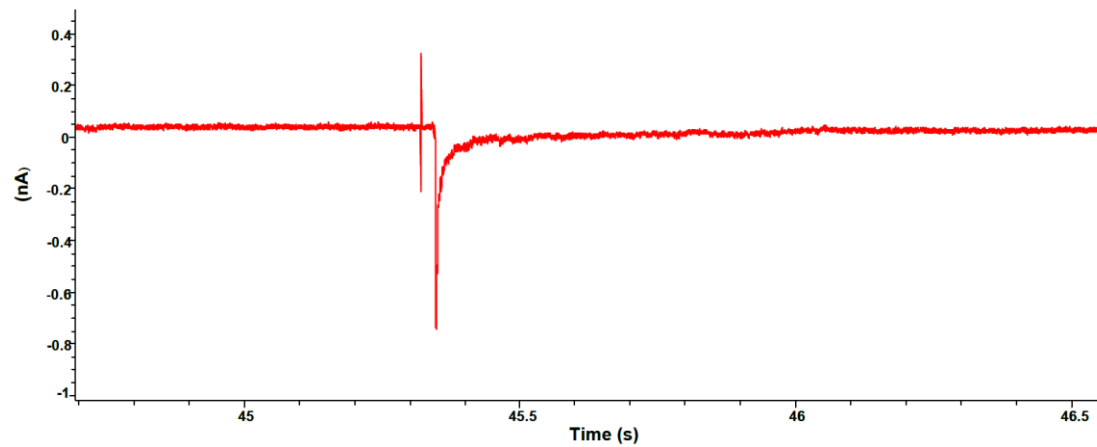
**hnAChR  $\alpha 7$ /ric3 Allosteric Modulation of Acetylcholine Induced Current, Blockade by Methyllycaconitine:** **Left:** The red trace shows approximately 800 pA of current induced by the application of 300  $\mu$ M acetylcholine alone. The black trace shows the same cell after washout of the acetylcholine followed by a 3 minute preincubation with 5  $\mu$ M PNU-120596 and then stimulation of the current by the co-application of 5  $\mu$ M PNU-120596 + 300  $\mu$ M acetylcholine. There was approximately 8.5 nA of a persistent inward current induced by the co-application of 5  $\mu$ M PNU-120596 + 300  $\mu$ M acetylcholine. (PatchXpress Data). **Right:** Currents induced by 300  $\mu$ M acetylcholine (AC) and 5  $\mu$ M PNU-120596 (PNU) (red bars) were blocked by the selective nAChR  $\alpha 7$  blocker 10  $\mu$ M methyllycaconitine (MLA) (blue bars). (PatchXpress Data).

BACK



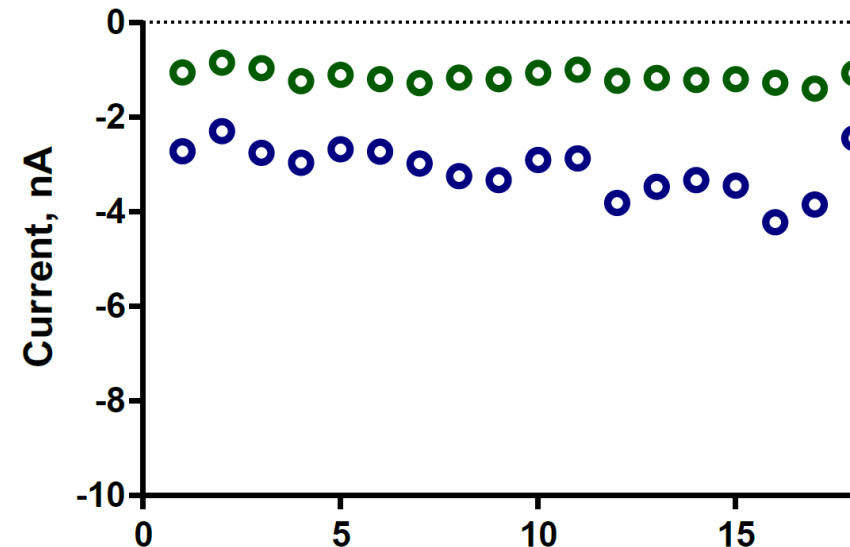
**hnAChR  $\alpha 7$ /ric3 Allosteric Modulation of Acetylcholine Induced Current, Stability of Expression and Seal Resistance over Passage:** **Left:** The partial allosteric modulator PNU-120595 increases the current activated by the addition of 300  $\mu$ M acetylcholine in a concentration-dependent manner. The peak inward current was approximately 6 nA and we found an  $EC_{50}$  of 926 nM and a Hill slope of 2.73. **Right:** Stability studies were performed determined by preincubating the cells with 5  $\mu$ M PNU-120596 for 3 minutes followed by the addition of 300  $\mu$ M acetylcholine + 5  $\mu$ M PNU-120596 at a holding potential of -60 mV. The blue line shows the percentage of cells expressing a mean peak inward current >4 nA at cell passages 13, 17, 21, 25, 28 and 30. The red bars show the mean seal resistance (mean  $\pm$  SD) for 8-14 cells per experiment. Functional expression of the hnAChR  $\alpha 7$ /ric3 currents was > 91% through 30 passages and the mean seal resistance was > 575 M $\Omega$ . (PatchXpress Data).

BACK



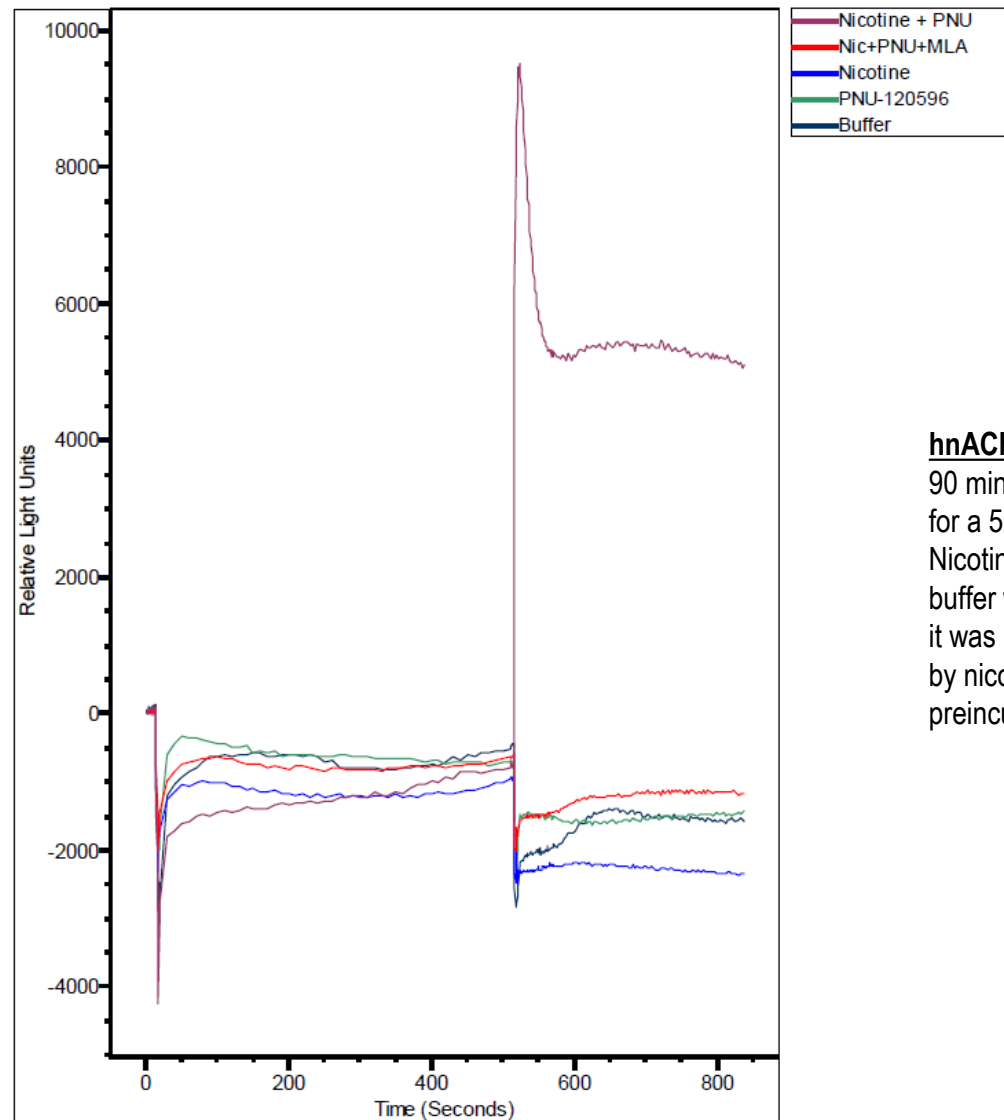
**hnAChR  $\alpha 7/\text{ric}3$  Other Agonist Activation:** **Left:** The response to epibatidine. The cells were treated with 100  $\mu\text{M}$  epibatidine, the cell responded with an inward current of approximately 700 pA. **Right:** The second figure shows the response to AR-R 17779. Here this cell responded to a challenge with 5  $\mu\text{M}$  AR-R 17779 with an inward current of approximately 950 pA (PatchXpress Data).

BACK



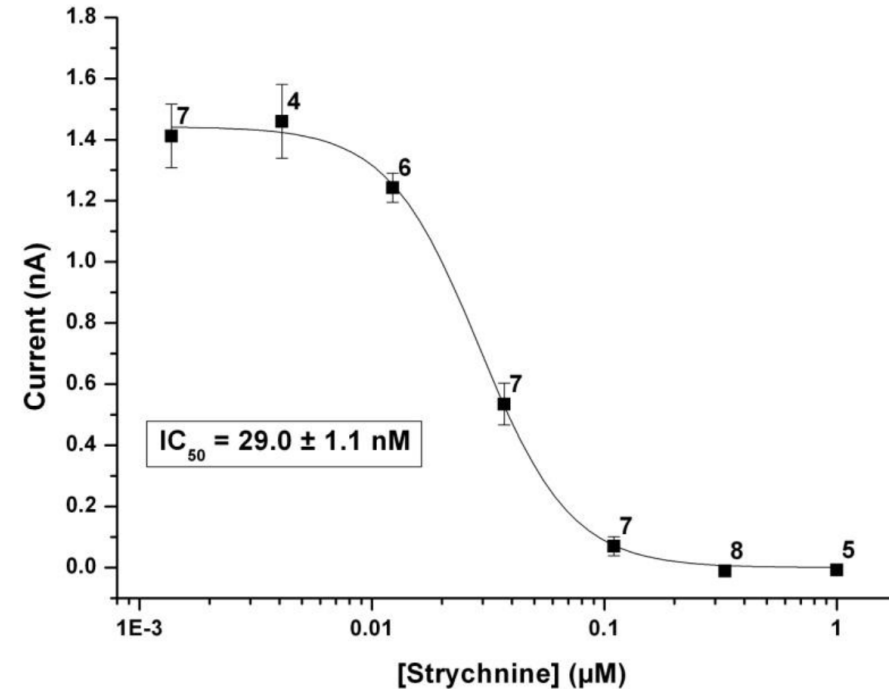
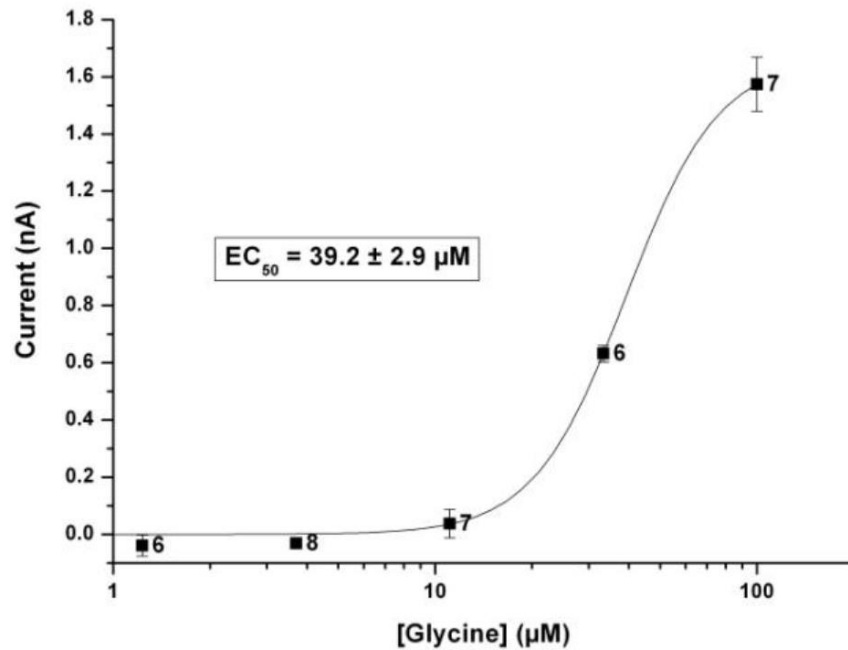
**hnAChR  $\alpha 7$ /ric3 Currents Measured on Port-A-Patch:** **Left:** To examine the reproducibility of currents elicited by repeated application of agonists or modulators, cells were held at -80 mV, and currents elicited by application of 300  $\mu$ M acetylcholine with 5  $\mu$ M PNU-120596 were elicited every 2 minutes. Each current trace was elicited by adding 5  $\mu$ M PNU-120596 for 500 ms, then adding 300  $\mu$ M acetylcholine with 5  $\mu$ M PNU-120596 for 100 ms, then washing with external solution for 6 seconds to allow the current to recover toward the baseline. The wash with external solution continued for an additional minute, then PNU-120596 was added for 30 seconds before eliciting the next current. Traces one and 18 are superimposed in the figure, and the red arrow points to trace 18. **Right:** The peak inward current amplitude, and the current integral, recorded for 38 minutes in the whole-cell configuration are shown in the green and blue symbols, respectively. (Port-a-Patch Data).

BACK



**hnAChR  $\alpha 7$ /ric3 Calcium Flux Data:** Cells were pre-loaded with the calcium indicator dye Fluo-8 (Alexa) at 30°C for 90 minutes. Following two wash cycles the cells were placed onto the instrument and the test compounds were added for a 520 seconds preincubation at the following final concentrations: methyllycaonitine = 10 $\mu$ M; PNU120-596 = 5 $\mu$ M. Nicotine was added at 520 seconds at final concentration of 100 $\mu$ M and data collected as graphed below. The external buffer was used as described in (7). The addition of nicotine alone (blue trace) either did not stimulate calcium influx or it was not detectable under these conditions. Preincubation with the positive allosteric modulator PNU-120596 followed by nicotine addition (maroon trace) did result in a large, sustained influx of calcium. This calcium flux was blocked by preincubation with the selective nAChR  $\alpha 7$  blocker methyllycaonitine (red trace). (FLIPR<sup>TETRA</sup> Data).

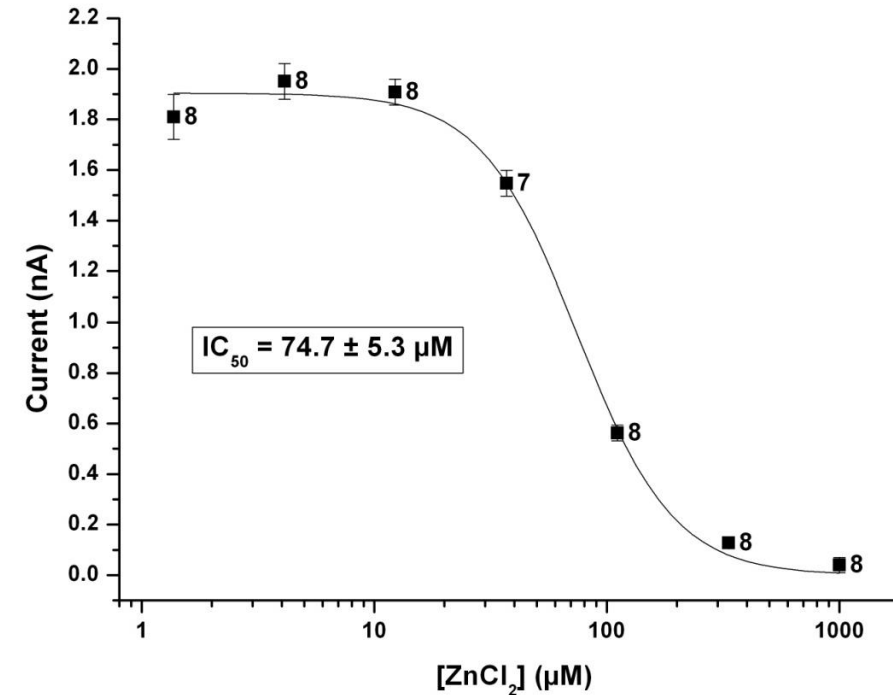
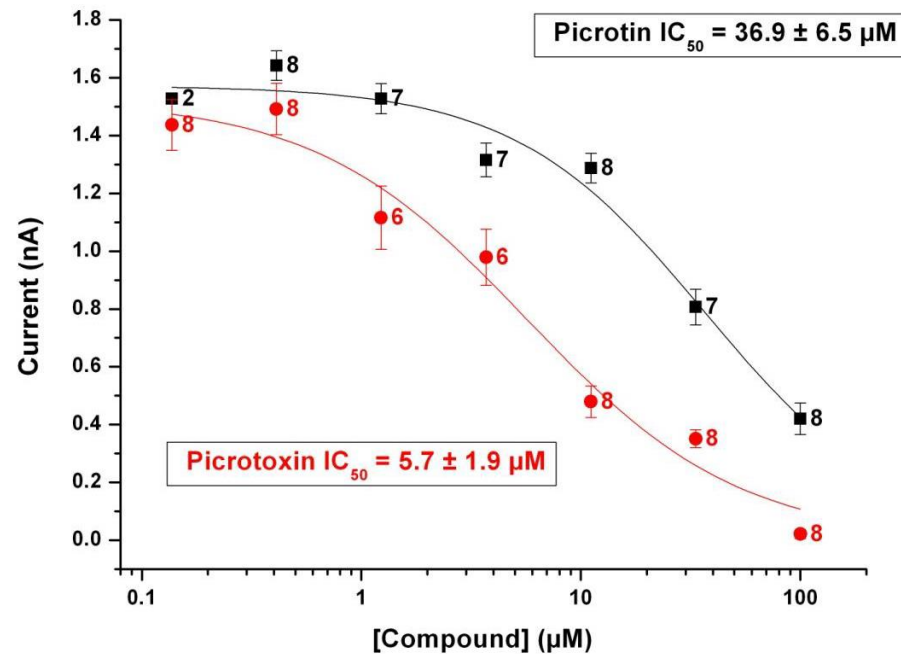
BACK



**hGlyRA1 Agonist and Antagonist Dose Response Curves:** **Left:** Increasing concentrations of glycine were added to separate patch-plate wells and the evoked outward current at 0 mV was measured. Glycine dose-dependently increased the outward current with an  $EC_{50}$  of 39  $\mu$ M. **Right:** Various concentrations of strychnine were incubated for 100 s and then in the presence of 100  $\mu$ M glycine. Strychnine dose-dependently inhibited glycine evoked outward currents with an  $IC_{50}$  of 29 nM. (IonWorks Quattro Data).

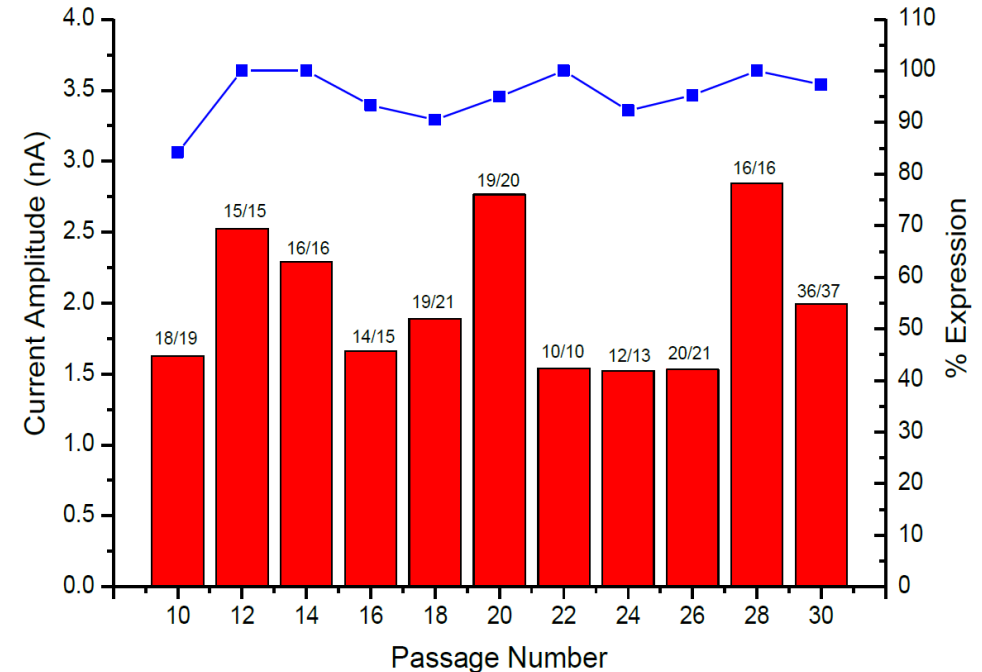
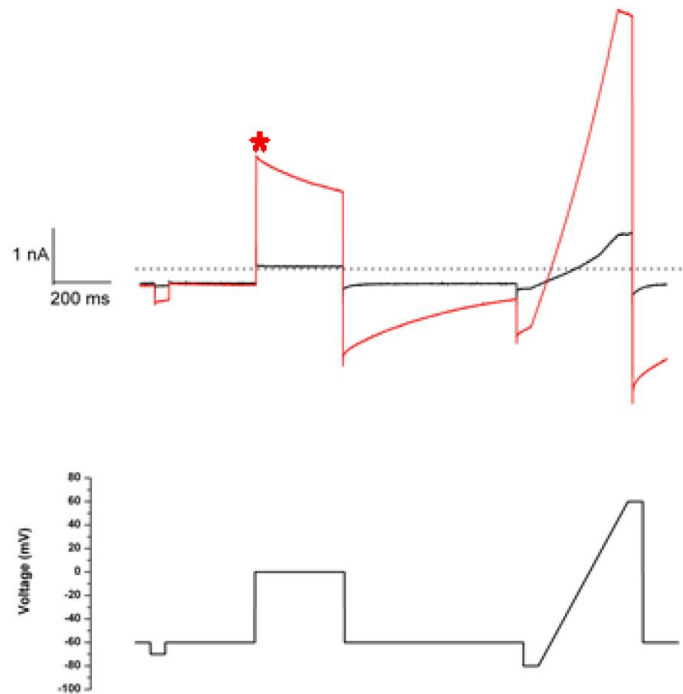


BACK



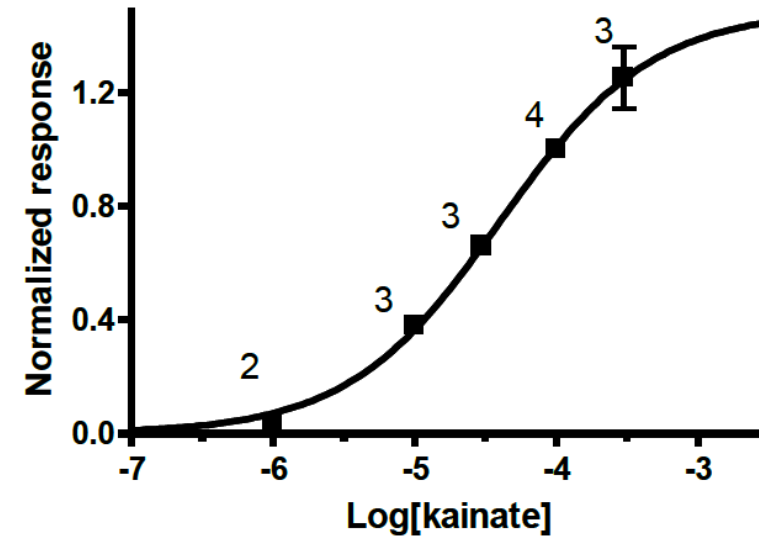
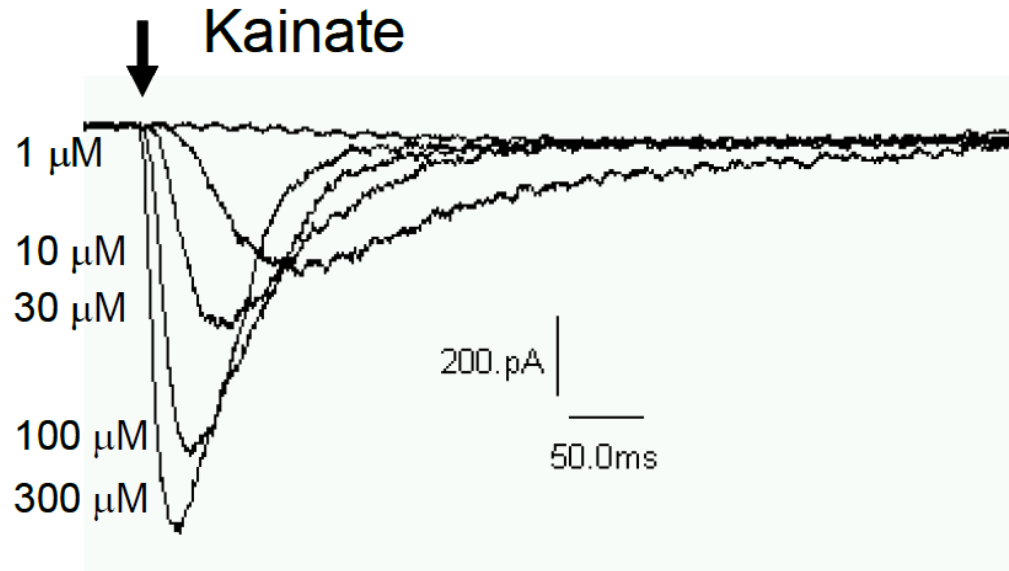
**hGlyRA1 Effect of Picrotoxin and Picrotin on Glycine-evoked Currents, Effect of  $\text{Zn}^{2+}$  on Glycine-evoked Currents:** Left: Various concentrations of compound were incubated for 100 s and then in the presence of 100  $\mu\text{M}$  glycine. Picrotoxin and picrotin dose-dependently inhibited glycine evoked outward currents with  $\text{IC}_{50}$  values of 5.7  $\mu\text{M}$  and 36.9  $\mu\text{M}$  respectively. Right: Various concentrations of  $\text{Zn}^{2+}$  were incubated for 100 s and then in the presence of 100  $\mu\text{M}$  glycine.  $\text{Zn}^{2+}$  dose-dependently inhibited glycine evoked outward currents with an estimated  $\text{IC}_{50}$  value of 74.7  $\mu\text{M}$ . Between 1 and 10  $\mu\text{M}$   $\text{Zn}^{2+}$  the mean outward current evoked by 100  $\mu\text{M}$  glycine was >1.8 nA whereas in the absence of  $\text{Zn}^{2+}$  the mean current was around 1.6 nA. (IonWorks Quattro Data).

BACK



**hGlyRA1 Glycine Evoked Currents on IonWorks HT, Stability of Expression over Passage:** **Left:** Typical current traces evoked before (black trace) and after (red trace) the application of 300  $\mu$ M Glycine. The zero current level is shown by the black dotted line. Voltage protocol shown below current trace. **Right:** The blue squares show the percentage of cells expressing mean current amplitude of  $\geq$  500 pA at 0 mV in response to 300  $\mu$ M glycine at cell passage 10 through to 30. The lower panel shows the mean current amplitude (red bars) and adjacent to these the number of these cells (number of cells expressing  $>$ 500 pA / number of cells sealing  $>$ 50 M $\Omega$ ). The maximum n-number was 24 cells for passages 10 through to 28 and 48 cells at passage 30 (IonWorks HT Data).

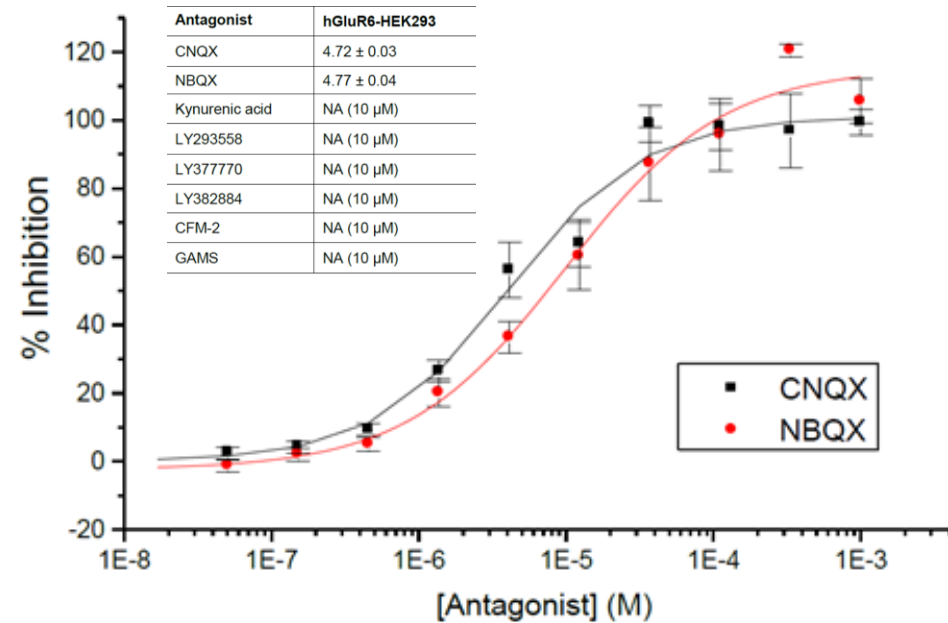
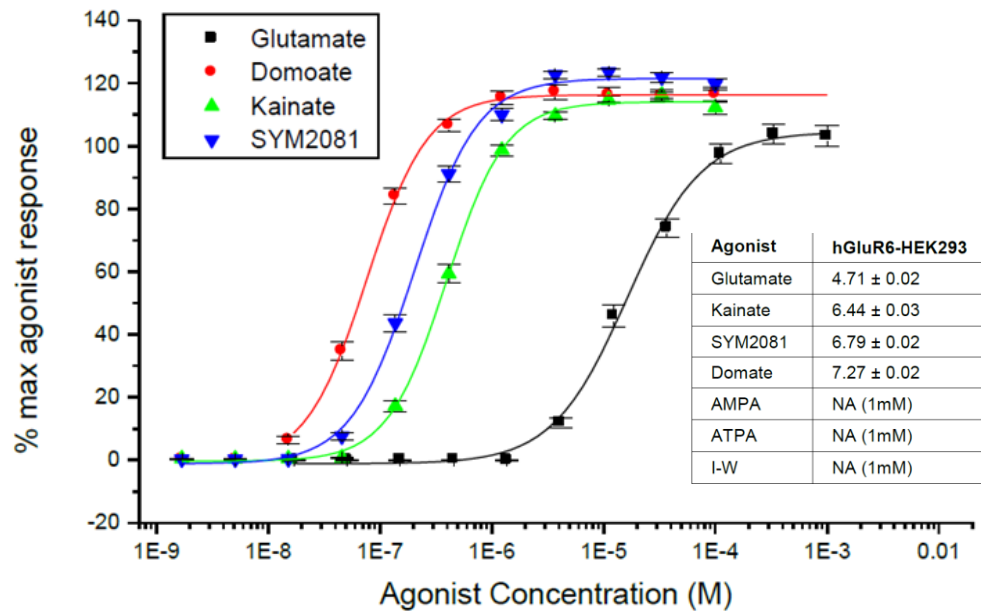
# GluR6 (CYL3049)



BACK

**Raw Kainate Currents and Agonist Activation:** (Left) Kainate-induced hGluR6 currents recorded from a single cell, activated by increasing concentrations of agonist applied for 1s starting as indicated by the arrow. (Right) Concentration-response curve for kainate-evoked currents. The x-axis shows the log concentration of kainate (M) and the y-axis the current amplitude normalized to the 100 μM evoked current amplitude value. Each point represents the mean value from the indicated number of determinations (different cells). From the four parameter logistic equation the pEC<sub>50</sub> value was 4.4 (EC<sub>50</sub> = 39.8 μM) and the Hill slope 0.8 (Manual Patch-Clamp Data).

BACK



**Agonist and Antagonist Pharmacology for GluR6:** (Left) To assess agonist pharmacology, four agonists with reported activity at hGluR6 were tested alongside three that were reported to be inactive against hGluR6 but active against hGRIK1. (Right) Data in Table 1 demonstrates that the agonist pharmacology is consistent with expression of the hGluR6 channel. The standard antagonists CNQX (6-cyano-7-nitroquinoxaline-2,3-dione) and NBQX (3-dihydroxy-6-nitro-7-sulfamoyl-benzo(f)quinoxaline) both blocked the response to 100 mM glutamate with a pIC50 value of 4.7 (FLIPR Data).